Palaeobiodiversity and Palaeoenvironments
https://doi.org/10.1007/s12549-025-00662-5

SENCKENBERG

ORIGINAL PAPER

A small vertebrate (Urodela, Anura, Squamata, Rodentia) assemblage from Fada Nana Cave (Quaternary, northern Italy)

Andrea Villa[1] · **Elisa Luzi**[2] · **Massimo Delfino**[1,3]

Received: 7 November 2024 / Revised: 2 May 2025 / Accepted: 13 May 2025
© The Author(s) 2025

Abstract

The Italian Peninsula is commonly interpreted as a Quaternary refuge, with a particularly important role for taxa requiring humid environments. This is testified by a relatively high diversity of amphibians on the peninsula nowadays, and also by the regional fossil record. Here we provide a complete description of the palaeoherpetofauna from Fada Nana Cave, in Verona province. It includes at least four amphibians (*Salamandra salamandra*, *Bufo* gr. *bufo*, *Bufotes* gr. *viridis*, *Rana temporaria*) and six reptiles (Lacertidae indet., *Anguis* gr. *fragilis*, *Zamenis* gr. *longissimus*, *Natrix* sp., *Vipera* gr. *aspis*, and an indeterminate small Colubroides) from Middle Pleistocene deposits. Fossils from Recent levels within the cave also reveal the presence of brown frogs and a green lizard, *Lacerta* gr. *viridis*. Rather interesting is the absence of the large anguid *Pseudopus*, found in other Early to Late Pleistocene-age sites in Veneto, and whose lack may be explained by the higher elevation of Fada Nana Cave. Based on the preliminary analysis of the small mammal assemblage, pre-Recent deposits in Fada Nana Cave are Middle Pleistocene in age and are tentatively assigned to the MIS 13 or 15 Interglacial, within the early Toringian Small Mammal Age. The Middle Pleistocene fauna recovered in the cave indicates a forested and moist environment, with water bodies and open meadows, for the nearby area.

Keywords Amphibians · Biochronology · Glaciations · *Pseudopus* · Reptiles

Introduction

Recent studies (Macaluso et al. 2021a, 2023a) highlighted the Italian territory as an important refugial area for amphibians during the Plio-Pleistocene climatic changes, adding a degree of complexity to the classical hypothesis of northern Mediterranean peninsulae (i.e. the Iberian, Italian and Balkan peninsulae) acting as southern refugia for organisms affected by cooling and aridization during the Quaternary glacial cycles (e.g. Hewitt 1996, 1999, 2000; but see Ratnikov 2024 for a different view). This is further evidenced not only by the high diversity of amphibians living in the Italian Peninsula nowadays (Sindaco et al. 2006; Lanza et al. 2007; Di Nicola et al. 2019), including several endemic taxa (e.g. the genus *Salamandrina*, two species of *Speleomantes*, *Lissotriton italicus*, and *Rana italica*), but also by a Pleistocene fossil record in Italy preserving remains of amphibian taxa that were once widespread in Europe, but later disappeared from the continent or even went completely extinct. Examples of this are remains of the discoglossid *Latonia* from the Early Pleistocene of Pietrafitta, in Umbria, representing one of the only two Quaternary occurrences of this frog genus in Europe and a new, potentially endemic species (Sorbelli et al. 2021, in prep.), as well as the albanerpetontids from Rivoli Veronese, in Veneto, which are currently the last global occurrences of this enigmatic clade (Delfino and Sala 2007; Villa et al. 2018a; note that López-García et al. 2024 mentioned a slightly older, though still undescribed, occurrence in northeastern Spain). The fossil record of the spectacled salamander, genus *Salamandrina*, also testifies for a Quaternary survival in continental Italy only, after a

This article is a contribution to the special issue "Festschrift for Márton Venczel"

✉ Andrea Villa
andrea.villa@icp.cat

[1] Institut Català de Paleontologia Miquel Crusafont (ICP-CERCA), Edifici ICTA-ICP, c/Columnes s/n, Campus de la UAB, 08193 Cerdanyola del Vallès, Barcelona, Spain

[2] Institut für Naturwissenschaftliche Archäologie, Eberhard Karls Universität, Hölderlinstraße 12, 72074 Tübingen, Germany

[3] Dipartimento di Scienze della Terra, Università degli Studi di Torino, Via T. Valperga Caluso 35, 10125 Torino, Italy

Published online: 19 June 2025

wider European distribution during the Neogene (Macaluso et al. 2021a, b).

Multiple reasons are most likely behind the role played by the Italian Peninsula as a refugium for amphibians during the Quaternary, but a more general explanation can be found in the wetter climate characterising it compared to the drier Iberia and the Balkans (Macaluso et al. 2023a; note: the climate of southeastern France, which is considered as part of the Italian geographic province by Lanza and Corti 1996, might have been more comparable to the Italian Peninsula). Such distinctly humid conditions were quantitatively reconstructed for at least Rivoli Veronese (Villa et al. 2018a), thus potentially supporting that environmental feature as favourable for the last albanerpetontids, as well as for *Speleomantes*, another unexpected amphibian occurrence from the same locality. The higher amount of humidity, which was particularly persistent throughout glacial and interglacial phases in northern Italy (Fauquette and Bertini 2003; Bertini 2010), may have also allowed the local survival of specific reptiles tied to more humid environments; e.g. the *Pseudopus pannonicus* lineage during the Early Pleistocene in Veneto (Villa et al. 2020a). This, together with other Late Pliocene and Pleistocene findings of amphibian and reptilian groups now absent from the current Italian fauna (e.g. *Pelobates syriacus*, *Mauremys*, and amphisbaenians: Delfino 2003; Blain et al. 2016; Collareta et al. 2020), implies that a comprehensive understanding of the recent past diversity of these animals in the country is pivotal to comprehend the current diversity and how it originated.

To provide additional data on the Italian Pleistocene herpetofauna, and in particular on northern Italian palaeoherpetological assemblages, we here report on the fossil amphibians and reptiles from the Quaternary deposits of Fada Nana Cave, in Verona province. Previously, amphibians and reptiles from this cave were only preliminary listed in a short summary of Plio-Quaternary herpetofaunas from the Veneto region by Delfino et al. (2008) and in a table reporting the same preliminary data by Villa et al. (2020a: table 2). No proper description of the remains was provided prior to our study. It is worth noting that most of the palaeoherpetological assemblage from Fada Nana Cave comes from a Middle Pleistocene paleosol, but a few fossils of a (sub)Recent age recovered in the same excavation campaign with the Pleistocene ones are also described herein. In this paper, we: 1) describe and identify the amphibian and reptile remains from Fada Nana Cave; 2) reconsider the age assessment for the pre-Recent portion of the assemblage by documenting its age-diagnostic rodents; 3) reconstruct the local Middle Pleistocene palaeoenvironment based on amphibian, reptile, and rodent species in the assemblage; and 4) evaluate what the assemblage from the cave contributes to our understanding of amphibian and reptile diversity during the Pleistocene in northern Italy.

Geological and chronological setting

Fada Nana Cave ("Grotta della Fata Nana" in Italian) is registered as "Buso della Fada Nana", nr. 7036 V VR in the "Catasto Grotte Veneto" list (http://www.catastogrotteveneto.it/Home/Wish). It is a small cavity located in Bosco Chiesanuova municipality (45° 35′ 49″ N, 11° 2′ 32″ E), in the Lessini Mountains (Fig. 1a). It extends for 11 m with a height of 2 m and a total downwards slope of 2 m. The entrance of the cave opens at 751 m asl, on the right slope of Vajo de Squaranto, a canyon-like valley. The east-facing wall of the valley is "about 10–80 m high and 400 m long. It consists of Jurassic limestone, with the superimposition of two types of rocks: the Rosso Ammonitico Veronese in the upper part and the Oolite di San Vigilio in the lower part" (Sauro and Zorzi 2017: p. 76). The entrance of the cave (Fig. 1c) is located in the southern sector of this wall, within the Oolite di San Vigilio. The cavity was part of a larger karstic system. It is possible to observe a closed continuation and a vertical chimney, probably connecting the cavity with others that developed vertically nearby (Sauro et al. 2007; Sauro and Zorzi 2017).

The Soprindentenza per i Beni Archeologici del Veneto coordinated archaeological excavation campaigns at Fada Nana Cave between the years 2000 and 2003 (Salzani and Sauro 2003). They investigated a 2 m-thick sequence that yielded lithic artifacts, ceramics, and bones dated between the Copper and the Modern ages (Sauro et al. 2007). Sauro et al. (2007) described a lower complex consisting of a highly concretionated Pleistocene paleosol with remains of fauna, including microvertebrates, seemingly unrelated to the rest of the sequence, which they named US 127 (orange and labelled "4" in Fig. 1b). The layer was reddish in colour, composed mainly of red clay transported inside after the erosion of terra rossa-type paleosols (Sauro and Zorzi 2017). After the archaeological layers were completely removed, Professor Benedetto Sala (Università degli Studi di Ferrara) was called to carry out the excavation of the lower complex in the years 2004 and 2005. Locations within the cave (either left or right wall) from where fossils were collected were noted by Sala's team and are herein reported. For some specimens, locations within the cave were not recorded; we report those as "unknown" in our inventories. The whole lower complex makes up a coherent assemblage with the same chronology (with the exception of a few, intrusive elements of a much younger, sub-Recent age, reported as "Recent" in the Systematic palaeontology section). The amphibians and reptile fossils reported herein were recovered during the 2004 campaign.

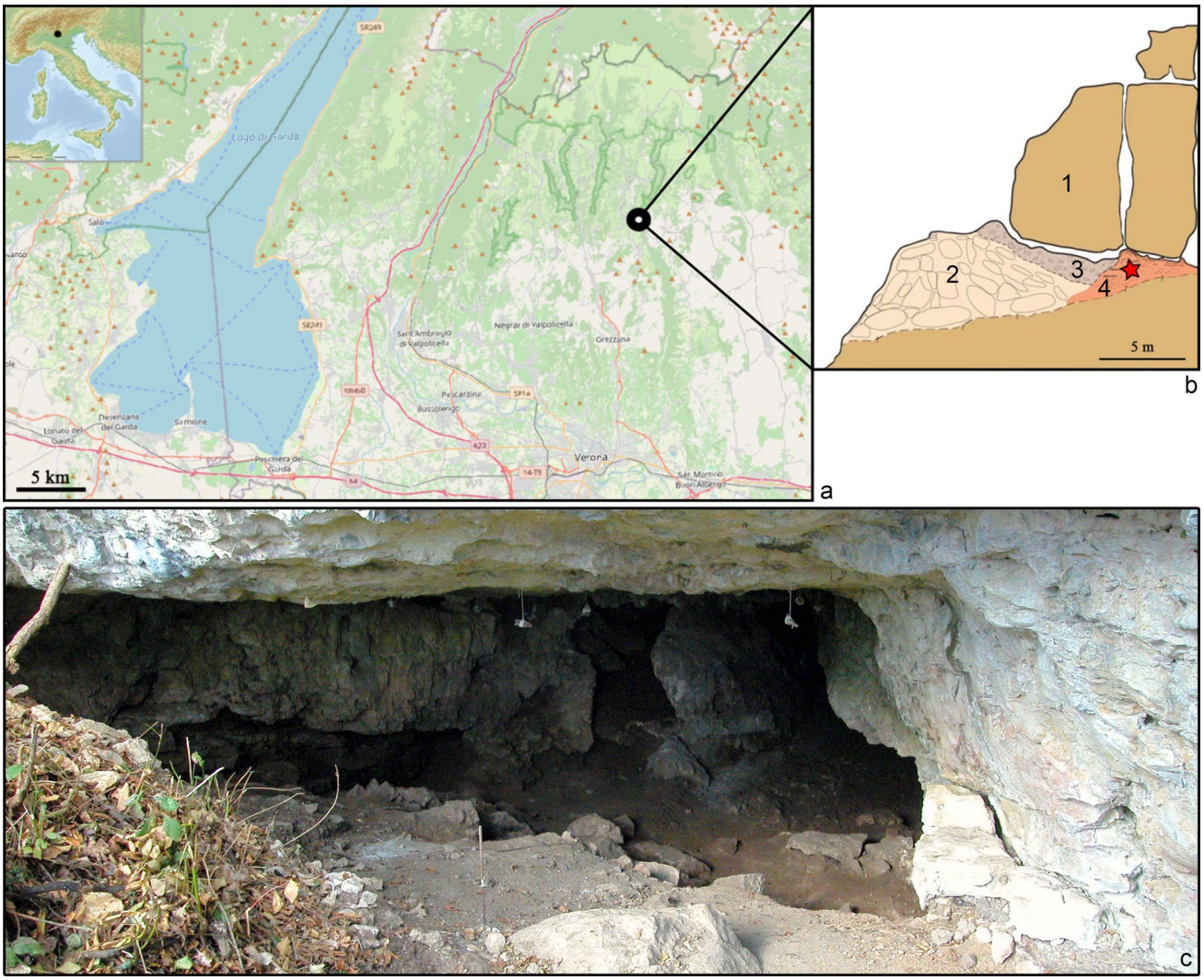

Fig. 1 Map and stratigraphic column of Fada Nana Cave, Verona Province, northern Italy. **a** Geographic location (black circle) of Fada Nana Cave. ©OpenStreetMaps (CC BY-SA 2.0), modified from Catasto Grotte Veneto. **b** Schematic stratigraphy of the cave area, modified from Sauro and Zorzi (2017); for a more detailed profile of the cave deposits, see Sauro et al. (2007: fig. 5). **c** Photo of the entrance of the cave at the time of excavations (picture by U. Sauro). Legend: *1* Oolite di San Vigilio; *2* collapsed blocks in front of the entrance of the cave; *3* archaeologic layers; *4* Pleistocene deposits (= "lower complex" in text). The star indicates the provenance of the palaeontological assemblage

Locatelli (2005) provided a preliminary list of the mammal species identified at Fada Nana Cave in the first phase of the research. Among micromammals, *Arvicola mosbachensis*, *Pliomys episcopalis*, *Microtus* (*Terricola*) *arvalidens*, and an archaic form of *Dinaromys* cf. *bogdanovi* were reported, whereas for the large mammals it is worth mentioning the finding of a maxillary fragment of *Macaca sylvanus* preserving deciduous teeth (Locatelli 2005). Updated lists of the rodents from Fada Nana Cave (based on data from Locatelli 2005, this study, and E.L., pers. obs; see also Supplementary Information SI1) include eight species of the subfamily Arvicolinae (*Arvicola mosbachensis*, *Clethrionomys glareolus*, *Dinaromys* cf. *bogdanovi*, *Pliomys coronensis*, *P. episcopalis*, *Microtus* cf. *agrestis*, *Microtus* cf. *arvalis*, *M.* (*Terricola*) *arvalidens*), one species of the subfamily Cricetinae (*Cricetulus bursae*), and two species of the subfamily Murinae (*Apodemus* spp.). Additionally, three species of the family Gliridae (*Eliomys* sp., *Glis glis*, and *Muscardinus* sp.) and two of the family Sciuridae (*Sciurus vulgaris* and *Marmota marmota*) are present.

Based on the presence of *Arvicola mosbachensis*, *Cricetulus bursae*, and *Pliomys episcopalis*, we can position the Fada Nana Cave assemblage in the Middle Pleistocene, specifically in the early Toringian Small Mammal Age (Sala and Masini 2007), starting approximately at 600 ka. The evolutionary stage of *A. mosbachensis* suggests that the

age of the Fada Nana Cave assemblage should be younger than Isernia la Pineta, which is dated to the end of MIS 15 (583–561 ka, $^{40}Ar/^{39}Ar$: Peretto et al. 2015). By contrast, the evolutionary stage of *Dinaromys* cf. *bogdanovi* suggests that the Fada Nana Cave assemblage is older than layers 39–27 of Visogliano, which are dated to MIS 12 (ca. 424–478 ka: Abbazzi et al. 2000; Falguères et al. 2008; Dalla Valle 2011). *Microtus* (*T.*) *arvalidens* might indicate an age close (either slightly older, slightly younger, or even the same age) to Visogliano. Teeth of *Glis glis* from Fada Nana Cave retain some archaic Biharian characters (see Supplementary Information SI1), which seems to agree with the stratigraphic position suggested by *Dinaromys*: that is, the assemblage is in the early phases of the early Toringian. Conservatively, based on the rodent assemblage, we can date the Middle Pleistocene deposits at Fada Nana Cave to between MIS 15 and MIS 12 inclusive.

Occurrences in Fada Nana Cave of *Macaca sylvanus*, *Glis glis*, *Sciurus vulgaris*, *Eliomys* sp. and *Muscardinus* sp. point to a mild climatic phase, with a substantial presence of temperate forest around the site (inference based on requirements for extant populations as reported by IUCN 2024). Furthermore, in the Italian Peninsula, the presence of *M. sylvanus* suggests temperate and wet climatic conditions (e.g. Mazza et al. 2005; Bona et al. 2016; Mecozzi et al. 2021). At Visogliano, *Macaca* sp. occurs in the lower layers of the shelter (Abbazzi et al. 2000), which are dated to MIS 13 (Falguères et al. 2008). Based on the presence of *Macaca* at Fada Nana Cave and its association with other taxa indicative of interglacial conditions, therefore, one could tentatively date the assemblage more precisely to an Interglacial stage; i.e. MIS 15 or 13.

Material and methods

The fossil material from Fada Nana Cave reported in this paper includes mostly isolated amphibian and reptile bones (labelled with the acronym GFN-HE, for "Grotta della Fata Nana", Herpetological material), plus a sample of selected rodent teeth and rare jaws (labelled with the acronym BFN_, for "Buso della Fada Nana") used to refine the biochronology of the site (see Supplementary Information SI1 for taxonomic descriptions of micromammal material). Although some specimens are bulk-numbered, all figured specimens bear unique specimen numbers. All fossils are stored in the collections of the Dipartimento di Biologia ed Evoluzione, Università degli Studi di Ferrara, Italy. Although all recovered amphibian and reptile bones are reported, we only figure examples of the most diagnostically significant elements. Amphibian and reptile bones were photographed with a Leica M205 microscope equipped with the Leica application suite v4.10 at the Università degli Studi di Torino. Drawings of micromammal teeth are based on photographs taken with a Leica EZ4 microscope at the Università degli Studi di Ferrara and modified with Photoshop. Anatomical terminology for amphibians and reptiles follows: Macaluso et al. (2020, 2023b) and Ratnikov and Litvinchuk (2007) for urodeles; Sanchiz (1998) and Gómez and Turazzini (2016) for anurans; Villa and Delfino (2019) and Čerňanský et al. (2019) for lizards; and Auffenberg (1963), as reported by Szyndlar (1984), for snakes. Anatomical terminology and measurements for rodent teeth follow: van der Meulen (1973) and Heinrich (1978) for arvicolines; Hír (1998) for cricetines; and Daoud (1993) for glirids.

Systematic palaeontology

Amphibia Blainville, 1816
Urodela Duméril, 1805
Salamandridae Goldfuss, 1820
Salamandra Garsault, 1764

Salamandra salamandra (Linnaeus, 1758)
(Fig. 2a–i)

Material: Right wall: one trunk vertebra (GFN-HE 0026), two caudal vertebrae (GFN-HE 0027 and 0028). Left wall: one caudal vertebra (GFN-HE 0103).

Description

Trunk vertebra: The large-sized trunk vertebra (Fig. 2a–e) has an opisthocoelous centrum that is about 6 mm long. The centrum has no distinct neck, and the anterior condyle is anteriorly flat, with no distinct inclination in lateral view. In the same view, the centrum displays a clear ventral concavity. The vertebra is partly covered by matrix, meaning some of the structures (such as the subcentral foramina, if present) are not clearly visible. Only the left transverse process (rib bearers sensu Ratnikov and Litvinchuk 2007) is partly preserved. It is posterolaterally directed. The posterior ventral crests are little developed, whereas the anterior ones are absent. The zygapophyseal crests are well developed. The neural arch is low and flat. It is broken at both its anterior and posterior margins. The remnants of a low neural crest (neurapophysis sensu Ratnikov and Litvinchuk 2007) are visible. The prezygapophyses are preserved. They are wide and horizontal. In dorsal view, the vertebra is wide.
Caudal vertebra: The caudal vertebrae (e.g. Fig. 2f–i) are comparable with the trunk vertebra in both morphology and size, even though the former are better preserved.
Remarks: The above-described salamandrid trunk vertebra can be referred to *Salamandra salamandra* because of its large size, low neural arch, low neurapophysis, little-developed ventral crest, and well-developed zygapophyseal crests (Ratnikov and Litvinchuk 2007; Macaluso et al. 2023b).

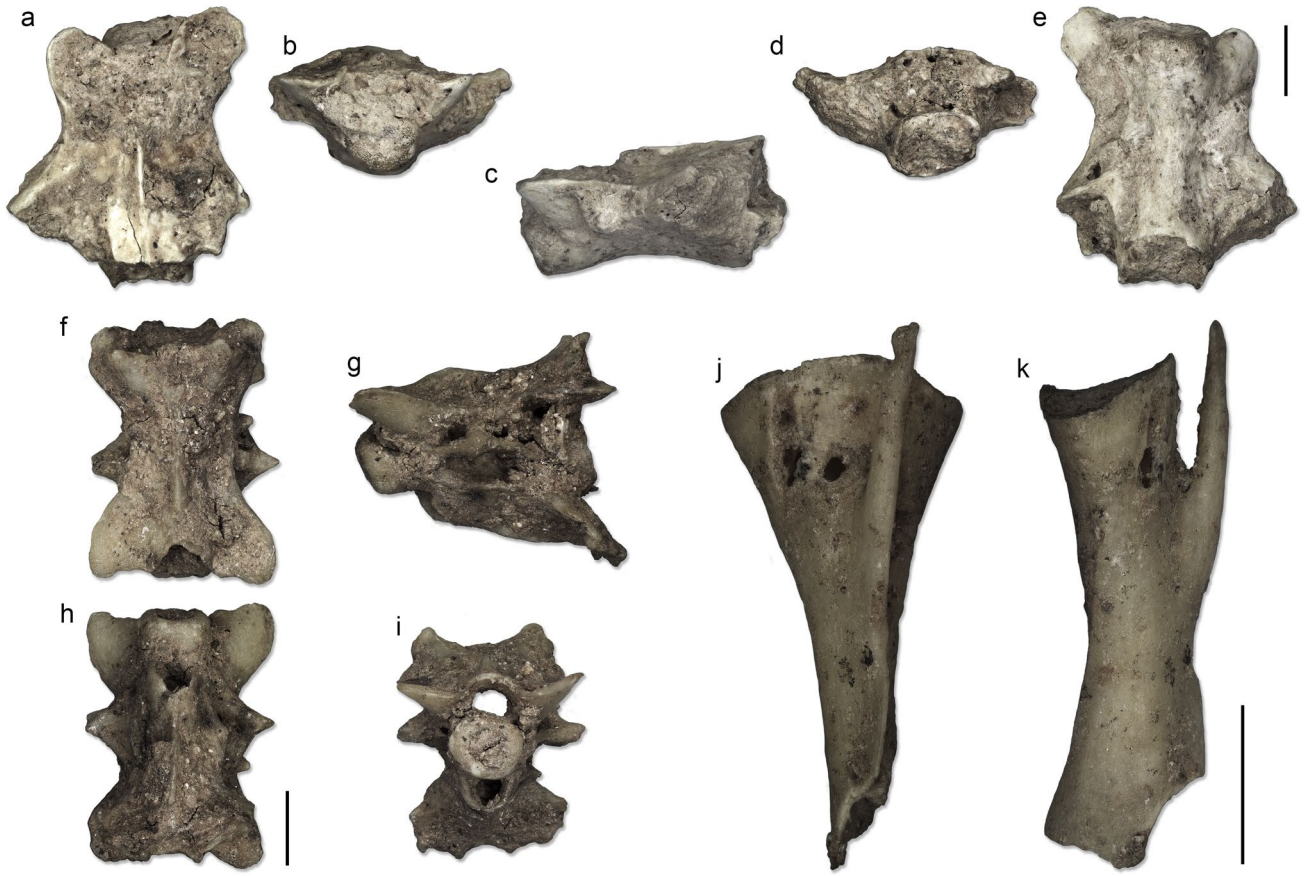

Fig. 2 Bones of urodeles from Fada Nana Cave. **a**–**e** trunk vertebra (GFN-HE 0026) of *Salamandra salamandra* in dorsal (**a**), anterior (**b**), left lateral (**c**), posterior (**d**) and ventral (**e**) views. **f**–**i** caudal vertebra (GFN-HE 0027) of *Salamandra salamandra* in dorsal (**f**), left lateral (**g**), ventral (**h**) and anterior (**i**) views. **j**, **k** left tibia (GFN-HE 0029) of Urodela indet. in dorsal (**j**) and anterior (**k**) views. Specimens at different magnifications; see corresponding 1 mm scale bars

Little is known about vertebral differences among the extant *Salamandra* species, but *S. salamandra* is the largest among the continental European species of the genus. Haller-Probst and Schleich (1994) reported that their sample of *Salamandra atra* had distinctly shorter vertebrae than *S. salamandra*. The other congener present in continental Europe, *Salamandra lanzai*, is only slightly larger than *S. atra*, not reaching the size of *S. salamandra* (Lanza et al. 2007). Because of this, we here favour attributing GFN-HE 0026 to *S. salamandra*. The caudal vertebrae can be assigned to the same taxon due to similar morphology and size. *Salamandra salamandra* is the only salamander currently living in the area (Sindaco et al. 2006).

Urodela indet.
(Fig. 2j, k)

Material: Right wall: one ilium (GFN-HE 0120), two tibiae (GFN-HE 0119 and 0029).

Remarks: The morphology and size of these remains is comparable with that of the respective bones in *Salamandra salamandra* (the only urodele currently identified in the assemblage). However, we here refer them only to indeterminate urodeles, because of the absence of clear diagnostic features due to the poor knowledge of the comparative osteology of *Salamandra* species and appendicular bones of European urodeles in general.

Some descriptive remarks on the tibiae are worth mentioning. The better-preserved one, GFN-HE 0029 (Fig. 2j, k), is medium sized. It lacks the distal end, and the total length of the preserved portion is 5 mm. It has a well-developed tibial crest that gives rise to a long, slender and pointed tibial spine. The tip of the tibial spine extends beyond the proximal margin of the tibia. The other tibia, GFN-HE 0119 (not figured), is less well preserved, but similar in size and shape.

Anura Duméril, 1805
Bufonidae Gray, 1825

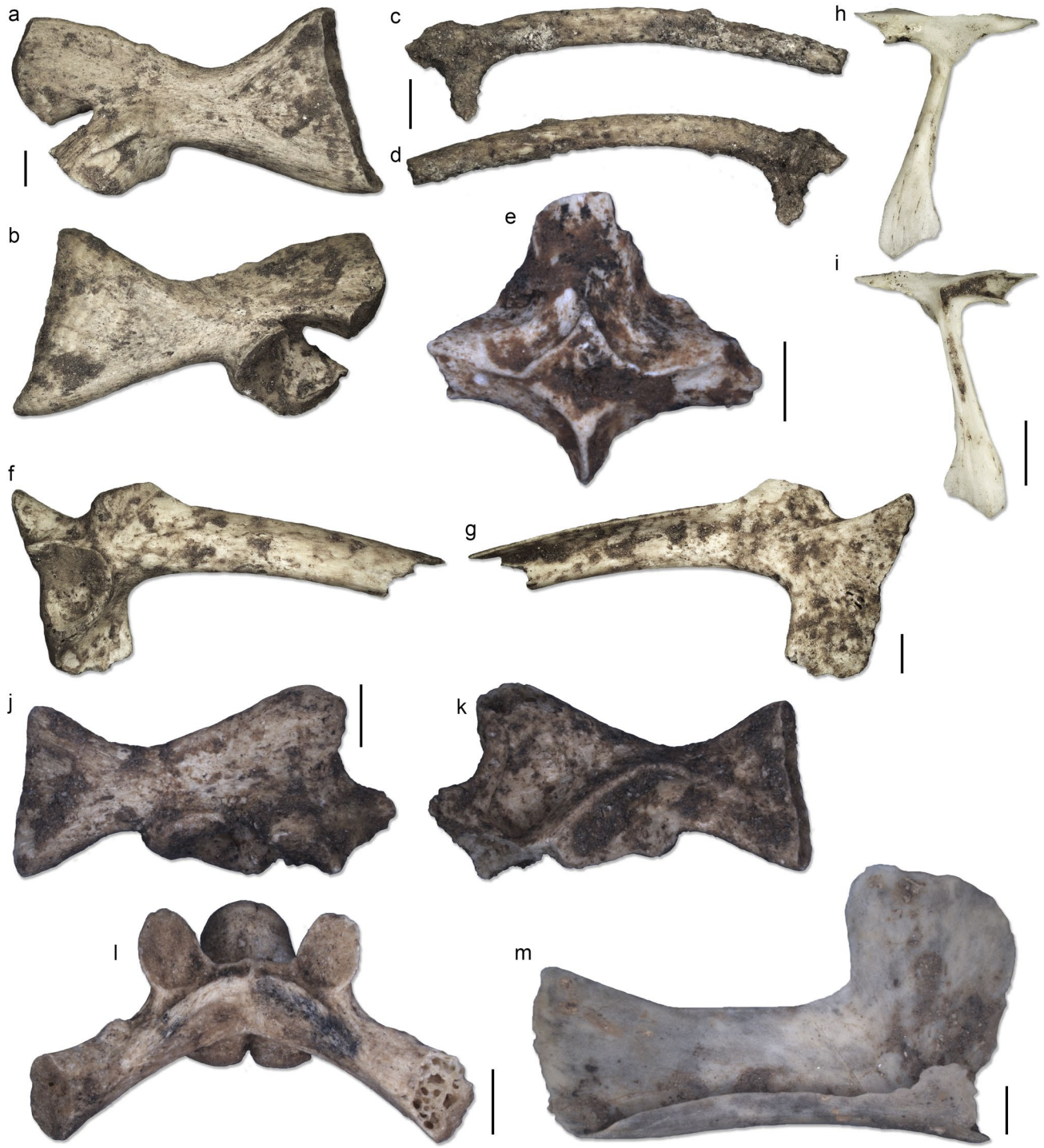

Fig. 3 Bones of anurans from Fada Nana Cave. **a**, **b** right scapula (GFN-HE 0037) of *Bufo* gr. *bufo* in dorsal (**a**) and ventral (**b**) views. **c**, **d** left ilium (GFN-HE 0042) of *Bufotes* gr. *viridis* in medial (**c**) and lateral (**d**) views. **e** parasphenoid (GFN-HE 0021) of Bufonidae indet. in ventral view. **f**, **g** right ilium (GFN-HE 0001) of *Rana temporaria* in lateral (**f**) and medial (**g**) views. **h**, **i** right squamosal (GFN-HE 0150) of *Rana* sp. in lateral (**h**) and medial (**i**) views. **j**, **k** right scapula and part of right coracoid (GFN-HE 0045) of *Rana* sp. in ventral (**j**) and dorsal (**k**) views. **l** sacral vertebra (GFN-HE 0156) of Ranidae indet. in dorsal view. **m** right suprascapula (GFN-HE 0039) of Anura indet. in ventral view. Specimens at different magnifications; see corresponding 1 mm scale bars

Bufo Garsault, 1764
Bufo bufo Linnaeus, 1758

Bufo gr. *bufo*
(Fig. 3a, b)

Material: Left wall: one atlas (GFN-HE 0064), two scapulae (GFN-HE 0037 and 0038), one femur (GFN-HE 0074).

Description

Atlas: The atlas (not figured) is relatively large and robust. It has two wide anterior cotyles, which are separated by a small spatium interglenoidale. The lateral ends of the cotyles are inclined dorsally at about 45° in anterior view. The posterior condyle is dorsoventrally compressed. The neural arch is relatively robust, defining a neural canal that is ogival in anterior view. Dorsally, the crista neuralis is present, but the arch is still partially unfused along the midline. In lateral view, there is no osseous expansion ("épine sous-zygapophysaire" sensu Bailon 1999) on the posterior margin of the lateral wall and below the postzygapophysis.
Scapula: The scapulae (e.g. Fig. 3a, b) are elongate, large and robust. The cavitas glenoidalis is well visible in ventral view, being ventrally directed. The supraglenoidal fossa is not present. The pars acromialis is robust and its margin is relatively angular, rather than rounded. Along the anterior margin of the scapula, a small ridge is visible on GFN-HE 0037 (Fig. 3a), whereas the ridge is more developed on GFN-HE 0038 (not figured).
Femur: GFN-HE 0074 (not figured) is a large and robust femur. It displays a well-developed crista femoris, which splits to form a triangular structure towards the proximal end.
Remarks: Following the diagnostic features reported by Bailon (1999), these remains can be assigned to the *Bufo bufo* species complex, which is still present in the area of Fada Nana Cave (Sindaco et al. 2006). The atlas differs from other European bufonids because of the ogival neural arch and the absence of expansions ventral to the postzygapophyses. As far as the scapulae are concerned, significant features are the absence of the supraglenoidal fossa and the presence of an anterior ridge. The femur can be referred to the same species complex due to its robustness and the distinctly split crista femoris.

Bufotes Rafinesque, 1815
Bufotes viridis (Laurenti, 1768)

Bufotes gr. *viridis*
(Fig. 3c, d)

Material: Left wall: one ilium (GFN-HE 0042).

Description

Ilium: The ilium (Fig. 3c, d) is relatively small and well preserved, but partially covered by matrix. It has no dorsal crest nor calamita ridge. The dorsal tubercle is rounded and bears two small lobes on its surface. The acetabular fossa is semicircular. Anterior to it, a deep preacetabular fossa is present. Despite being encrusted with matrix, the medial surface of the bone appears relatively flat. The dorsal acetabular expansion is broken.
Remarks: The presence of *Bufotes* gr. *viridis* in the assemblage is testified by a single ilium characterised by the absence of dorsal crest, presence of a bilobed dorsal tubercle and a deep preacetabular fossa, and no calamita ridge (Bailon 1999). Green toads are currently present in the area (Sindaco et al. 2006; Di Nicola et al. 2019).

Bufonidae indet.
(Fig. 3e)

Material: Right wall: one parasphenoid (GFN-HE 0021), one trunk vertebra (GFN-HE 0020), one humerus (GFN-HE 0126). Left wall: two maxillae (GFN-HE 0111 and 0112), nine trunk vertebrae (GFN-HE 0063), one clavicle (GFN-HE 0065), six humeri (GFN-HE 0072 and 0073).

Description

Maxilla: The maxillae (not figured) are moderately large and robust. They have a trapezoidal shape in lateral view, with a squared anterior end and a pointed posterior end. Medially, the lamina horizontalis is well developed and laminar. The processus palatinus is represented by a low ridge. Posteriorly, there is no processus zygomaticomaxillaris. The crista dentalis is completely toothless. The lateral surface of the bone is smooth.
Parasphenoid: GFN-HE 0021 (Fig. 3e) is a fragmentary parasphenoid that is large and robust. Posteriorly, it bears a short but well-developed processus posterior, which is pointed. All other processes (i.e. the pars medialis anteriorly and the partes laterales laterally) are broken off. Only their wide bases are preserved. A complex of strongly developed ridges is present on the ventral surfaces of the posterior process, the partes laterals, and at the junction of these processes.
Trunk vertebra: The trunk vertebrae (not figured) are large and robustly built. The procoelous centrum is well developed and the lateral walls of the neural arch are robust. The robust transverse processes are laterally directed and arise posterior to the prezygapophyses.
Clavicle: The clavicle (not figured) is large, robust and straight.

Humerus: Humeri (not figured) are large. The largest ones are robust, but smaller humeri are gracile. The shaft is straight. The eminentia capitata is spherical (sometimes less ossified distally; e.g. GFN-HE 0126) and aligned with the main axis of the bone. The fossa cubitalis ventralis is deep. No specimen displays the crista paraventralis, whereas the well-developed crista ventralis is visible on the best preserved specimens. The cristae medialis and lateralis are poorly developed. The epicondylus medialis is well developed and robust. The epicondylus radialis is smaller. On the dorsal surface, the olecranon scar is large.
Remarks: The above-reported bufonid bones can be assigned only to indeterminate members of the family. According to Bailon (1999), characters supporting the bufonid referral of these bones are: toothless maxillae; a robustly-built parasphenoid with a short processus posterior and well-developed ridges on the ventral surface; procoelous trunk vertebrae with transverse processes not located ventral to the prezygapophyses and robust lateral walls of the neural arch; a large, robust and straight clavicle; straight humeri devoid of crista paraventralis and provided with a laterally-shifted eminentia capitata, a deep fossa cubitalis ventralis, and poorly developed cristae medialis and lateralis. The size and the robustness of these bones suggest those pertain to the larger *Bufo* gr. *bufo* and not to the smaller *Bufotes* gr. *viridis*, but this cannot be clearly ascertained.

Ranidae Batsch, 1796
Rana Linnaeus, 1758

Rana temporaria Linnaeus, 1758
(Fig. 3f, g)

Material: Right wall: two ilia (GFN-HE 0032). Left wall: one ilium (GFN-HE 0001).

Description

Ilia: The three ilia (e.g. Fig. 3f, g) are moderately large and relatively well preserved. They have a distinct dorsal tubercle that is elongate, has a rugose lateral surface and is continuous anteriorly with the dorsal crest. The crest is moderately high and bent medially. The acetabular fossa is semielliptical. Dorsal to the latter and posterior to the dorsal tubercle, there is a small supracetabular fossa. The dorsal acetabular expansion is well developed. It creates an obtuse angle with the tubercle. The ventral acetabular expansion also is well developed. The medial surface of the ilial body is relatively flat, with no distinct iliac groove or tubercle. In posterior view, the ilioischiatic juncture is narrow.
Remarks: These ilia are assigned to *Rana temporaria* because of the following features (Gleed-Owen 1998; Bailon 1999; Blain and Arribas 2017): presence of a moderately high dorsal crest, which bends medially; well-developed dorsal acetabular expansion; absence of iliac groove and iliac tubercle; and narrow ilioischiatic juncture. In combination with these features, the rugosities on the lateral surface of the dorsal tubercle also support assignment to *R. temporaria*, because this is one of the species of brown frogs with a rugous dorsal tubercle (Ratnikov 2001; Villa et al. 2021). *Rana temporaria* is currently present in the area (Sindaco et al. 2006).

Rana sp.
(Fig. 3h–k)

Material: Right wall: two scapulae (GFN-HE 0019 and 0116). Left wall: four scapulae (GFN-HE 0045 and 0046). Left wall (Recent): one squamosal (GFN-HE 0150).

Description

Squamosal: The squamosal (Fig. 3h, i) is medium-sized. It has a T-shape, with a long and spatulate ramus zygomaticus, whereas the anterior and posterior portions of the transverse branch are shorter and similar in size to one another. The transverse branch is not expanded to form a laminar structure. The inner ridge is moderately developed.
Scapula: The scapulae (e.g. Fig. 3j, k) are elongate and moderately large. There are no ridges on the anterior margin. The cavitas glenoidalis opens posteriorly, being partially hidden by the pars acromialis in ventral view. In dorsal view, the pars glenoidalis display a robust ridge that continues onto the main body of the bone. In at least some specimens (e.g. GFN-HE 0045; Fig. 3j, k), portions of other bones of the pectoral girdle are still articulated with the scapula.
Remarks: These remains pertain to an indeterminate brown frog. Following Bailon (1999), the squamosal is attributed to *Rana* due to complete absence of an alar lamina, overall T shape, similar-sized portions of the transverse branch, and spatulate ramus zygomaticus. The scapulae can be referred to *Rana* because of the elongate shape, the absence of the anterior ridge, the morphology of the cavitas glenoidalis, and the presence of an inner ridge that develops on the main body of the bone (Bailon 1999). For the Middle Pleistocene scapulae, these might belong to the only brown frog species recognised so far in the assemblage, namely the common frog *R. temporaria*. Being of more Recent age, the squamosal could pertain to any of the brown frog species that currently live in the area where Fada Nana Cave is located (i.e. *R. dalmatina*, *R. latastei*, and *R. temporaria*: Sindaco et al. 2006; Sillero et al. 2014; Speybroeck et al. 2016; Di Nicola et al. 2019), but this cannot be clearly established in absence of more diagnostic remains.

Ranidae indet.
(Fig. 3l)

Material: Right wall: one trunk vertebra (GFN-HE 0016), one urostyle (GFN-HE 0018), one femur (GFN-HE 0017). Left wall: three angulars (GFN-HE 0043), five trunk vertebrae (GFN-HE 0061), three sacral vertebrae (GFN-HE 0062 and 0156), two femora (GFN-HE 0040), four tibiofibulae (GFN-HE 0048). Left wall (Recent): one parasphenoid (GFN-HE 0151).

Description

Parasphenoid: The parasphenoid (not figured) is moderately large. The pars medialis is long and lanceolate. The partes laterales are slightly narrower than the pars medialis. The tips of the partes laterales are broken, but they slightly enlarge distally. The processus posterior is triangular and moderately short. The ventral surface of the junction of the four branches composing the parasphenoid is smooth.
Angular: The angulars (not figured) are slender and display a well-developed and almost vertical processus coronoideus.
Trunk vertebra: The trunk vertebrae (not figured) vary from slenderly built to moderately robust. The centrum is procoelous. The neural arch is short, and it has thin lateral walls and a low carina neuralis. The posterior end of the neural arch roof is not pointed. The transverse processes are thin, laterally directed and placed posterior to the prezygapophyses.
Sacral vertebra: The sacral vertebrae (e.g. Fig. 3l) are moderately robust. They have an anterior condyle, two posterior rounded condyles, and cylindrical and posterolaterally directed transverse apophyses.
Urostyle: The urostyle (not figured) is moderately large and robust. It has two subcircular anterior cotyles and a high crista dorsalis. The anterior part of the neural arch is broken.
Femur: The femora (not figured) are moderately large and slender. They have no crista femoris.
Tibiofibula: The tibiofibulae (not figured) have a straight anterior margin and a concave posterior margin. They are large and slender. The ends are only slightly larger than the diaphysis.
Remarks: The above-reported bones can be only attributed to indeterminate ranids. Based on the criteria reported by Bailon (1999), these are: a parasphenoid provided with a lanceolate pars medialis and a distinct processus posterior; angulars with an almost vertical processus coronoideus; procoelous trunk vertebrae with a short neural arch, thin lateral walls, transverse processes located posterior to the prezygapophyses, and a carina neuralis dorsally; sacral vertebrae with an anterior condyle, two posterior condyles, and cylindrical transverse apophyses; urostyle with two subcircular anterior cotyles and a high crista dorsalis; slender femora with no crista femuris; and large and slender tibiofibulae. Just like the Middle Pleistocene remains assigned to *Rana* sp., these fossils may pertain to *R. temporaria*, except maybe for the parasphenoid GFN-HE 0151. This latter bone is more Recent in age and most likely belongs to the same taxon as the squamosal GFN-HE 0150 from the same layer (see above).

Fig. 4 Bones of *Lacerta* gr. *viridis* from Fada Nana Cave. **a**, **b** left frontal (GFN-HE 0152) in dorsal (**a**) and ventral (**b**) views. **c**, **d** right compound bone (GFN-HE 0153) in lateral (**c**) and medial (**d**) views. Specimens at different magnifications; see corresponding 1 mm scale bars

Anura indet.
(Fig. 3m)

Material: Right wall: one angular (GFN-HE 0131), one urostyle (GFN-HE 0130), two radioulnae (GFN-HE 0030 and 0132), 19 indeterminate elements (GFN-HE 0031 and 0129). Left wall: two premaxillae (GFN-HE 0059 and 0081), one sphenethmoid (GFN-HE 0099), one squamosal (GFN-HE 0055), one prootic-exoccipital (GFN-HE 0053), one trunk vertebra (GFN-HE 0058), two fragmentary vertebrae (GFN-HE 0051), one urostyle (GFN-HE 0050), three sternal elements (GFN-HE 0054), two suprascapulae (GFN-HE 0039 and 0052), seven coracoids (GFN-HE 0044 and 0060), one humerus (GFN-HE 0047), four radioulnae (GFN-HE 0049), one ischium (GFN-HE 0057), 41 indeterminate elements (GFN-HE 0041, 0056, and 0098).

Remarks: These remains are either too poorly preserved or non-diagnostic and are here referred only to indeterminate anurans. The largest and more robust specimens (e.g. the suprascapula GFN-HE 0039: Fig. 3m) might pertain to *Bufo* gr. *bufo*, which is the largest anuran recognised in the fossil assemblage.

Squamata Oppel, 1811
Lacertidae Oppel, 1811
Lacerta Linnaeus, 1758
Lacerta viridis (Laurenti, 1768)

Lacerta gr. *viridis*
(Fig. 4)

Material: Left wall (Recent): one frontal (GFN-HE 0152), one compound bone (GFN-HE 0153).]

Description

Frontal: The frontal (Fig. 4a, b) is well preserved. It is slightly more than 11 mm in length. In dorsal view, only a slight middle constriction is visible, with the lateral margin being almost parallel with the medial margin along the middle portion of the bone. At the anterior end, the lateral process is bifid, whereas the medial process is missing. The articular surface with the nasal is large and U-shaped, whereas the articular surface with the maxilla is reduced. Well-developed dermal sculpturing covers the dorsal surface of the bone. The groove separating the frontal and the frontoparietal shields is located about three-fifths of the distance posteriorly along the length of the specimen. The posterolateral process is short and distally rounded. The posterior margin is distinctly interdigitated. Laterally, the articular surface with the prefrontal and the postfrontal are far from each other, with the former being notably larger than the latter. The crista cranii is relatively wide, rises anteriorly, and gives rise to the long and slender anterior process. On the ventral surface of the bone, the articular surface with the parietal tables is visible.
Compound bone: The compound bone (Fig. 4c, d) is large. It is well preserved, missing only the distal tip of the retroarticular process. The surangular and prearticular/articular portions are still unfused in the anterior half of the bone. In medial view, the ventral margin of the bone is straight. The adductor fossa is anteroposteriorly elongate and wide. The articular condyle is subquadrangular and bears a robust tubercle on the dorsomedial corner. Despite the absence of the tip, the triangular shape of the retroarticular process is still recognisable. The lateral surface displays the anterior surangular foramen near the anterior end of the bone and the posterior surangular foramen near the articular condyle. The articular surface for the elongate angular is also visible. No distinctly developed longitudinal ridge is visible laterally.

Remarks: These two fossils clearly pertain to lacertids based on the following features (Villa and Delfino 2019): elongate frontal with a bifid lateral process, a long and slender anterior process, and an interdigitated posterior margin; elongate compound bone without angular process and provided with an articular surface for the angular, a wide adductor fossa, and a posteriorly-directed and triangular retroarticular process. The size of GFN-HE 0152 is comparable to that of a large-sized lacertid lizard, falling into the ranges of *Lacerta* and *Timon* among European species (Villa and Delfino 2019). The distinct posterior interdigitations and the reduced articulation surface with the maxilla are also comparable with the frontal morphology of these two genera (Barahona and Barbadillo 1997; Villa and Delfino 2019). Čerňanský (2010) stated that the groove separating the frontal and the frontoparietal ornamented shields is located at one-half of the total length of the frontal in the ocellated lizard *Timon lepidus*, whereas the groove is located at about three-fifths or even three-quarters of the length in species of *Lacerta*. However, this groove can be located at three-fifths of the length in some *T. lepidus* (Villa and Delfino 2019). Because of this variation, the position of the groove in GFN-HE 0152 cannot clearly exclude assignment to *T. lepidus*. Nevertheless, *T. lepidus* reaches significantly larger sizes compared to *Lacerta* species (frontal length of *T. lepidus* up to 21 mm: Villa and Delfino 2019; A.V., pers. obs.). *Timon lepidus* is currently not present in northeastern Italy, whereas a member of the *Lacerta viridis* group, *Lacerta bilineata*, still inhabits the area (Sindaco et al. 2006; Sillero et al. 2014; Speybroeck et al. 2016; Di Nicola et al. 2019). Because of this and its Recent age we here favour an attribution to the green lizards for this frontal. Adults of *Lacerta* species display an unconstricted frontal, with parallel lateral and medial margins at midlength (Barahona and Barbadillo 1997, 1998; Čerňanský and Syromyatnikova 2019; Villa and Delfino 2019), but the constriction is present in juveniles. The slight middle constriction showed by GFN-HE 0152 suggests it might pertain to a subadult. Even without considering the fact that the individual to which the frontal belonged could have reached a slightly larger size, GFN-HE 0152 is longer than the frontals of *Lacerta agilis* (frontal length of *L. agilis* up to about 8 mm: Villa and Delfino 2019). The 11 mm length of GFN-HE 0152 falls within the range of frontals of adults/subadults of the other *Lacerta* species. For those reasons, GFN-HE 0152 is here referred to *Lacerta* gr. *viridis*. The compound bone coming from the same level as this frontal is here tentatively assigned to the same taxon, because the incomplete fusion of the portions composing the bone suggest it belongs to a subadult individual of a large lacertid.

Lacertidae indet.
(Fig. 5)

Fig. 5 Bones of indeterminate lacertids from Fada Nana Cave. **a**, **b** right frontal (GFN-HE 0012) in dorsal (**a**) and ventral (**b**) views. **c**, **d** parietal (GFN-HE 0144) in dorsal (**c**) and ventral (**d**) views. **e**, **f** parietal (GFN-HE 0145) in dorsal (**e**) and ventral (**f**) views. **g**, **h** premaxilla (GFN-HE 0083) in anterior (**g**) and posterior (**h**) views. **i**, **j** left maxilla (GFN-HE 0015) in lateral (**i**) and medial (**j**) views. **k**, **l** left jugal (GFN-HE 0140) in lateral (**k**) and medial (**l**) views. **m**, **n** left pterygoid (GFN-HE 0013) in dorsal (**m**) and ventral (**n**) views. **o**, **p** right dentary (GFN-HE 0003) in lateral (**o**) and medial (**p**) views. **q**, **r** left lower jaw (GFN-HE 0080) in lateral (**q**) and medial (**r**) views. Specimens at different magnifications; see corresponding 1 mm scale bars

Material: Right wall: one frontal (GFN-HE 0012), two maxillae (GFN-HE 0014 and 0015), one pterygoid (GFN-HE 0013), 10 dentaries (GFN-HE 0008). Left wall: five frontals (GFN-HE 0143), three parietals (GFN-HE 0144, 0145, and 0149), two premaxillae (GFN-HE 0082 and 0083), 13 maxillae (GFN-HE 0077 and 0078), five jugals (GFN-HE 0139 and 0140), three pterygoids (GFN-HE 0142, 0146, and 0148), 32 dentaries (GFN-HE 0003, 0075, and 0076), three coronoids (GFN-HE 0141 and 0147), one compound bone (GFN-HE 0138), one articulated lower jaw (GFN-HE 0080).

Description

Frontal: The most informative example, GFN-HE 0012 (Fig. 5a, b) is a relatively well-preserved right frontal. Its total length slightly exceeds 8.5 mm. Dorsally, it bears

relatively well-developed dermal sculpturing, composed of a frontal shield anteriorly and a frontoparietal shield posteriorly. The groove between the shields is visible roughly at two-thirds of the total length from the anterior end. In dorsal view, the frontal is weakly constricted at midlength and becomes slightly wider towards the anterior end. The anterior end presents a large and U-shaped articulation surface for the nasal. The articulation surface with the maxilla appears strongly reduced. Anteriorly, both the lateral and the medial processes are mostly missing due to breakage. The posterolateral process is well developed and distally rounded. The posterior margin of the frontal is moderately interdigitated. In lateral view, the articulation surface with the prefrontal is large and reaches midlength, whereas the articulation surface with the postfrontal is small. These articulation surfaces do not contact each other. Ventrally, the crista cranii is low posteriorly, but deepens anteriorly. The area bearing the anterior process is broken. The other frontals (not figured) are morphologically similar, but generally less well preserved.

Parietal: The three parietals are fragmentary. GFN-HE 0144 (Fig. 5c, d) preserves most of the parietal table (mainly missing the right posterolateral corner of the table), whereas the other specimens are represented by one of the posterolateral corners of the bone. They are all small; e.g. the parietal table of GFN-HE 0144 is roughly 5.5 mm wide and roughly 5.5 mm long. However, these measurements are probably slightly lower than the actual size, because the specimen is not intact. The size of GFN-HE 0145 (Fig. 5e, f) is comparable, whereas GFN-HE 0149 (not figured) was likely slightly larger. The parietal table of GFN-HE 0144 is completely covered by well-developed dermal sculpturing, which clearly reaches the posterior margin of the table. The sculpturing is separated by grooves into two frontoparietal, one interparietal, two lateral, and an occipital shields. The last is moderately small. An elliptical parietal foramen is visible in the middle of the anterior half of the interparietal shield. A similar dermal sculpturing is also present on the other parietals, being represented only by one of the lateral shields. Dermal sculpturing also reaches the posterior margin of the bone in these specimens. The anterior margin of GFN-HE 0144 is poorly preserved, but a certain degree of interdigitation is still visible. On the ventral surface, the ventral crests are moderately wide and distinctly developed. The posterolateral ventral crests are not in clear contact with the anterolateral ones in GFN-HE 0144, whereas the contact is visible in GFN-HE 0145 (cf. Fig. 5d vs. f). The highly fragmentary nature of GFN-HE 0149 means the relative position of its ventral crests cannot be seen. The parietal fossa, preserved only in GFN-HE 0144, is wide and U-shaped. There is no parietal notch. Preserved intact in GFN-HE 0145, the left supratemporal process is moderately long, slender and pointed.

Premaxilla: The two premaxillae are small. The length of the alveolar border is 2.5 mm or smaller. The teeth are pleurodont, slender, cylindrical and closely spaced. The tooth crowns are generally badly preserved, but both a monocuspid tooth and a bicuspid one seem to be recognisable in the better preserved premaxilla, GFN-HE 0083 (Fig. 5g, h). The number of tooth positions is eight in GFN-HE 0082 (not figured) and nine in GFN-HE 0083. The ascending nasal process is relatively short and wide, and is leaf shaped in anterior view. The anterior surface is smooth, but a light hint of dermal sculpturing is visible in GFN-HE 0083 near the dorsal tip of the bone (the corresponding portion in the other specimen is missing). The posterior surface of the nasal process bears a well-developed septonasal crest, which reaches the dorsal tip. The palatal processes are relatively short and separated at the midline by a wide notch. Laterally, deep articulation surfaces for the maxillae are visible.

Maxilla: GFN-HE 0015 (Fig. 5i, j) is a small maxilla, 9 mm in total preserved length, and is split into two portions. This specimen is poorly preserved. The anterior premaxillary process shows a well-developed and pointed anterolateral process and a U-shaped anterior notch. The anteromedial process is broken, but it seems that a lappet could have been present on its dorsal surface. The facial process is largely missing, but an arched ridge is visible on its medial surface. The preserved portion of the lateral surface of the facial process displays poorly developed dermal sculpturing, at least in its anterior part. Ventral to this sculpturing, some ventrolateral foramina are present. The posterior process of the maxilla is broken. The posteriorly incomplete tooth row preserves at least 16 tooth positions. Preserved teeth are slender, cylindrical, closely spaced and pleurodont. The tooth crowns are relatively eroded, but a bicuspid condition with a small anterior accessory cusp is recognisable for at least some crowns. The other maxillae (not figured) share the same morphology with GFN-HE 0015, even though they are less well preserved. Teeth share the same morphology with those of the former specimen and they clearly show the bicuspid condition. GFN-HE 0078 (not figured) has a well-preserved anterior premaxillary process, which shows a distinctly developed lappet on the anteromedial process.

Jugal: Jugals (e.g. Fig. 5k, l) are small. They all have a well-developed quadratojugal process. Medially, the palatal process is well developed, but it does not bear a distinct medial process. A wide articular surface for the maxilla almost completely covers the anterior portion of the anterior process of the jugal. That articular surface recalls the stepped morphology of the posterior process of the maxilla. A pointed anterior end of the anterior process is (at least partially) preserved only in GFN-HE 0140 (Fig. 5k, l). Although never completely preserved, the posterodorsal process is relatively slender in all specimens. The lateral surface of the jugals displays weakly developed dermal sculpturing

only in the largest specimens, whereas that surface is smooth in the other specimens.

Pterygoid: The largest pterygoid, GFN-HE 0013 (Fig. 5m, n), lacks most of the quadrate process and the tip of the palatine process. The length of the preserved portion is slightly less than 7 mm. The palatine process is moderately wide and straight. It hosts a patch of pterygoid tooth positions on its ventral surface, but no teeth are preserved. It seems that the teeth were organised in two rows. The pterygoid flange is short, pointed and moderately robust. It bears a low ridge on its ventral surface and a well-developed ridge on its dorsal surface. Taking into account the missing portion of the palatine process, the pterygoid recess is deep. The preserved portion of the quadrate process displays a subcircular fossa columellae dorsally and a flat basipterygoid fossa medially. It is not clear whether a well-developed pterygoid ridge was present or not. The other pterygoids are smaller, but morphologically similar. Where the palatine process is preserved (i.e. all specimens but the unfigured GFN-HE 0146), the patch of pterygoid teeth also is present in these specimens. In contrast with GFN-HE 0013 and the other pterygoids, GFN-HE 141 (not figured) displays a well-developed ridge on the ventral surface of the pterygoid flange. The pterygoid ridge is not developed in the three smallest pterygoids.

Dentary: Isolated dentaries are abundant and all are moderately small (e.g. Fig. 5o, p). The best preserved and largest dentaries are roughly 8 mm in length. The posterior end of the bone (including the posterior portion of the tooth row) is always missing, but the rest of the bone is well preserved for at least some specimens. The subdental shelf is narrow and hosts a subdental ridge dorsally. The mandibular symphysis is narrow and horizontal. The Meckelian fossa is wide and narrows anteriorly. Counting from the anterior end, the opening of the alveolar canal is located by the 18th tooth position (GFN-HE 0003: Fig. 5o, p) or between the 18th and the 19th positions in the best preserved and largest specimens. However, the opening is located by the 16th position in the smaller GFN-HE 0075 (not figured). The ventral margin of the bone is convex in medial view. The anteriormost nineteen tooth positions, plus a small part of a twentieth one, are present in the best-preserved specimen, GFN-HE 0003 (Fig. 5o, p). Teeth are pleurodont, cylindrical and closely spaced. They are slender but tend to slightly increase in robustness posteriorly. Tooth crowns are either bicuspid or tricuspid. The lateral surface of the dentary is smooth, with five mental foramina. The other dentaries are morphologically comparable to GFN-HE 0003.

Coronoid: The coronoids (not figured) are small. They have a dorsally rounded coronoid process, which is relatively vertically developed. The labial process is relatively short anteroposteriorly and pointed. The anteromedial process is never completely preserved, but it is long. The posterior portion of the bone is badly preserved in all specimens, but at least one of them (GNF-HE 0147) bears a small, distinct and triangular posterior process. Medially, there is a well-developed coronoid ridge. Another ridge links the posterior margin of the coronoid process to the posterior portion of the bone.

Compound bone: GFN-HE 0138 (not figured) is a fragment of a small compound bone, represented only by the posterior end. The retroarticular process is triangular in medial view. It has a truncated posterior end and a smooth lateral surface. Ventrally, the retroarticular process is not expanded and so the ventral margin of the specimen is straight. The articular condyle is partially broken off.

Articulated lower jaw: GFN-HE 0080 (Fig. 5q, r) is a moderately complete lower jaw, missing the symphyseal region anteriorly and most of the compound bone posteriorly. The total preserved length of the specimen is 12 mm, whereas the preserved tooth row is 5.5 mm long. The morphology of the dentary, the coronoid, and the dentition are like those described above for the isolated elements. At least 15 dentary tooth positions are preserved. The splenial is elongate and blade-like, with a large anterior inferior foramen. The anterior mylohyoid foramen is not visible. The posterior portion of the coronoid is broken off. The anteromedial process of the coronoid is long. The angular is elongate and relatively wide. It hosts a foramen on its ventromedial surface. The adductor fossa is wide. On the lateral surface of the preserved portion of the compound bone, the anterior surangular foramen stands out ventral to the coronoid and there is a sharp longitudinal ridge dorsal to the angular.

Remarks: All these bones share a similar size range and are from a smaller-sized lacertid lizard. At least some specimens display adult features, supporting the presence of a smaller-sized lacertid in the assemblage. Examples of these adult features are (Barahona and Barbadillo 1997, 1998; Villa and Delfino 2019): well-developed dermal sculpturing on the skull roofing bones; sculpturing reaching the posterior margin on the parietals; presence of dermal sculpturing on at least one premaxilla and on the largest jugals; presence of pterygoid teeth; vertical coronoid process of the coronoid; and, if correctly interpreted, also the possible bicuspid crown in the premaxilla GFN-HE 0083. However, a more precise identification of the bones at the species or even genus level within Lacertidae is complicated by contrasting information given by different skeletal elements. The best-preserved frontal (GFN-HE 0012) displays a reduced articular surface with the maxilla as in some species of *Algyroides* and *Iberolacerta*, all *Lacerta* species, *Timon lepidus*, and *Zootoca vivipara* (Barahona and Barbadillo 1997; Villa and Delfino 2019). Nevertheless, it cannot be referred to either *Lacerta* or *T. lepidus*, because of the smaller size of the frontal and the groove in the dermal sculpturing is located at two-thirds of the length of the bone (Čerňanský 2010; Villa and Delfino 2019). *Lacerta* is further excluded by the moderate middle constriction. *Iberolacerta cyreni* and *Iberolacerta monticola*

have more developed posterior interdigitations (Villa and Delfino 2019) than those displayed by GFN-HE 0012, but it is not clear whether the moderately interdigitated posterior margin of the studied fossils is real or a taphonomic artifact. As for the parietals, slender supratemporal processes are found in several lacertid species (Villa and Delfino 2019), including *Acanthodactylus erythrurus*, *Algyroides marchi*, *Algyroides moreoticus*, *Dinarolacerta mosorensis*, *Eremias arguta*, *Iberolacerta bonnali*, *Ophisops elegans*, *Podarcis siculus*, *Psammodromus hispanicus*, and *Z. vivipara*. However, among these species, the Fada Nana Cave frontals can only pertain to *A. moreoticus*, *I. bonnali*, and *P. siculus* because of the following features (Villa and Delfino 2019): elongate shelf (contra *A. erythrurus*, *E. arguta*, *O. elegans*, and *Z. vivipara*); well-developed sculpturing (contra *A. erythrurus*, *E. arguta*, and *O. elegans*); sculpturing reaching the posterior margin of the shelf (contra *A. erythrurus*, *O. elegans*, *Ps. hispanicus*, and *Z. vivipara*); presence of an unreduced occipital shield (contra *A. erythrurus*, *E. arguta*, and *O. elegans*); large and U-shaped parietal fossa (contra *D. mosorensis* and *E. arguta*); and no parietal notch (contra *A. erythrurus*, *A. marchi*, *O. elegans*, *Ps. hispanicus*, and *Z. vivipara*). The presence of a lappet on the anteromedial process of the maxillae excludes these bones from *A. erythrurus*, two species of *Algyroides* (*Algyroides fitzingeri* and *A. marchi*), *E. arguta*, *Hellenolacerta graeca*, and *O. elegans* (Barahona and Barbadillo 1997; Villa and Delfino 2019), but it does not give further taxonomic insights. The stepped morphology of the maxillary posterior process, evidenced by the shape of the articular surface on the jugals, suggests a possible attribution of these latter bones to *I. monticola monticola*, *Lacerta*, or *Podarcis* (Barahona and Barbadillo 1997; Villa and Delfino 2019; Čerňanský 2025, this issue), but the first taxon is excluded by the presence of dermal sculpturing. *Lacerta* might also be excluded by the small size of the jugals. Some taxonomic information also is provided by pterygoids and compound bones. Pterygoids bearing teeth and a deep pterygoid recess are found in two species of *Algyroides* (*Algyroides nigropunctatus* and *A. moreoticus*), *Dalmatolacerta oxycephala*, *E. arguta*, *Lacerta*, and several *Podarcis* species (Barahona and Barbadillo 1997; Villa and Delfino 2019). The absence of a ventral expansion prevents attribution of the compound bones to both *A. erythrurus* and *E. arguta* (Barahona and Barbadillo 1997; Villa and Delfino 2019). In agreement with the size of the supposed adult specimens recognised among the fossils from Fada Nana Cave, all the above-mentioned bones suggest the presence of one or more small-sized lacertid species. The possibility of multiple species being present is supported by different skeletal elements implying contrasting taxonomic identifications (e.g. frontals vs. jugals). Only the premaxillae are not convincingly from a small-sized species. The short and leaf-shaped ascending nasal process is a characteristic feature of the larger-sized *Lacerta* species and *T. lepidus*, and of the small-sized *Z. vivipara* (Barahona and Barbadillo 1997; Čerňanský and Syromyatnikova 2019; Villa and Delfino 2019). However, premaxillae of *Z. vivipara* are generally smaller than those described herein and lack bicuspid teeth (Barahona and Barbadillo 1997; Villa and Delfino 2019). The premaxillae could therefore suggest the presence of small individuals of a larger-sized species, but it has to be noted that a more leaf-shaped process is sometimes present in large individuals of medium-sized species (e.g. *Podarcis muralis*: MGPUT MDHC 311 in the Massimo Delfino Herpetological Collection of the Museo di Geologia e Paleontologia of the Università degli Studi di Torino; A.V., pers. obs.). The identification of lacertid remains coming from the Middle Pleistocene levels of Fada Nana Cave is, therefore, complex, and it seems likely that more than one species of varying sizes could be represented in the fossil material. However, we also must acknowledge that the osteology of some lacertid species currently living in Eastern Europe is still poorly known and that the lacertid remains coming from Fada Nana Cave might pertain to a still unrecognised extinct species. Taking all of this into account, we here prefer to follow a cautious approach by identifying these remains as pertaining to indeterminate lacertid lizards, most likely belonging to one or more small-sized species. This material was previously reported as cf. *Podarcis* sp. by Delfino et al. (2008; identification subsequently reprised by Villa et al. 2020a: table 2), but given the information provided by the new comparisons presented herein, we discard even a tentative generic attribution for the time being.

Anguidae Gray, 1825
Anguinae Gray, 1825
Anguis Linnaeus, 1758
Anguis fragilis Linnaeus, 1758

Anguis gr. *fragilis*
(Fig. 6)

Material: Right wall: five trunk vertebrae (GFN-HE 0022 and 0024), one cloacal vertebra (GFN-HE 0023), three caudal vertebrae (GFN-HE 0025 and 0125). Left wall: two maxillae (GFN-HE 0104 and 0105), three dentaries (GFN-HE 0100–0102), 54 trunk vertebrae (GFN-HE 0002, 0066, and 0067), four cloacal vertebrae (GFN-HE 0069), 26 caudal vertebrae (GFN-HE 0070), two osteoderms (GFN-HE 0071).

Description

Maxilla: GFN-HE 0105 (Fig. 6a, b) is complete, whereas GFN-HE 0104 (not figured) is fragmentary. Our description is therefore based mainly on the former. The maxillae are small (GFN-HE 0105 is slightly less than 5 mm long) and slender. Anteriorly, the anterior premaxillary process is composed of long anteromedial and anterolateral processes separated by a wide and deep notch.

Fig. 6 Bones of *Anguis* gr. *fragilis* from Fada Nana Cave. **a**, **b** left maxilla (GFN-HE 0105) in lateral (**a**) and medial (**b**) views. **c**, **d** left dentary (GFN-HE 0100) in lateral (**c**) and medial (**d**) views. **e**–**i** trunk vertebra (GFN-HE 0002) in anterior (**e**), dorsal (**f**), right lateral (**g**), ventral (**h**) and posterior (**i**) views. **j**–**n** trunk vertebra (GFN-HE 0024) in anterior (**j**), dorsal (**k**), right lateral (**l**), ventral (**m**) and posterior (**n**) views. Specimens at different magnifications; see corresponding 1 mm scale bars

A well-developed lappet is present on the dorsal surface of the anteromedial process. The facial process is subtrapezoidal in lateral or medial outline, with a concave anterior margin, a convex dorsal margin, and a concave posterior margin. Medially, a low arched ridge is visible on the ventral portion of the process. The lateral surface of the facial process is smooth. Four ventrolateral foramina are visible. The posterior process is long and slender. The superior dental foramen is wide. Teeth are subpleurodont, well-spaced, canine-like, curve posteriorly and bear a pointed tip. Nine tooth positions are visible in GFN-HE 0105.

Dentary: Dentaries are small and slender. They reach up to 6 mm in total length. Medially, the Meckelian fossa is covered for most of its length by a smooth subdental shelf (i.e. without a subdental ridge). In GFN-HE 0100 (Fig. 6c, d), a small splenial spine is visible at the level between the eighth and the ninth tooth positions. Teeth are subpleurodont, canine-like and well-spaced. The pointed tip bends posteriorly. In all specimens, the total number of tooth positions cannot be counted, either due to the tooth row being broken or because of sediment cover. GFN-HE 0100 bears at least 10 tooth

positions. In the same specimen, the opening for the alveolar foramen is located by the ninth tooth position. The posterior portion of the intramandibular septum is free. The Meckelian fossa is narrow and opens ventrally. The ventral margin of the dentary is straight in medial view. The posterior end of the bone is broken in all fossils, but it clearly bends dorsally in GFN-HE 0101 (not figured). A short coronoid process is preserved in the same specimen. The mandibular symphysis is narrow and slightly dorsally inclined. Its posterior portion is slightly expanded medially. The lateral surface of the bone is smooth, with a few mental foramina.

Trunk vertebra: Trunk vertebrae (e.g. Fig. 6e–n) are small and slender, reaching up to 4 mm in centrum length. Centra are procoelous, dorsoventrally compressed and have a flat ventral surface and parallel lateral margins. The synapophyses are anterodorsally elongate. The neural arch has a distinctly developed neural spine. The zygapophyses are wide and dorsally inclined at about 45°. The neural canal is subtrapezoidal and roughly as tall as or slightly lower than the anterior cotyle in anterior view. GFN-HE 0067 (not figured) is associated with a small, thin and rounded osteoderm, the only visible surface of which is the smooth inner surface.

Cloacal vertebra: The cloacal vertebrae (not figured) share the same overall morphology of the trunk vertebrae, but they are slightly shorter and provided with two well-developed and ventrolaterally-directed transverse processes.

Caudal vertebra: Caudal vertebrae (not figured) have a dorsoventrally compressed and procoelous centrum, provided with fused hemapophyses. They have long and pointed transverse processes and dorsally bear a neural spine. The zygapophyses are suboval and dorsally inclined at about 45°. Except for the anteriormost caudals, the autotomy plane is usually present, even though it appears completely fused in the largest vertebrae. All caudals are small and slenderly built.

Osteoderm: The osteoderms (not figured) are small, thin and rounded. The external surface displays a smooth anterior portion and a vermicular sculpturing.

Remarks: These remains are assigned to *Anguis* gr. *fragilis* based on the following criteria (Klembara 1981; Holman 1998; Delfino et al. 2011; Klembara et al. 2014; Čerňanský et al. 2019; Villa and Delfino 2019): small size; subpleurodont, canine-like, posteriorly-bending and well-spaced teeth; free posterior portion of the intramandibular septum; dorsally-bending posterior end of the dentary (at least in GFN-HE 0101); dorsoventrally compressed vertebral centrum with parallel lateral margins; vertebral neural canal not taller than anterior cotyle; small, thin, and rounded osteoderms with no keel externally. The *Anguis fragilis* species complex, currently represented in the area by *Anguis veronensis*, includes all extant European *Anguis* species (Gvoždík et al. 2010, 2013), which are not distinguishable based on our poor knowledge of their comparative osteology (Villa et al. 2017; Villa and Delfino 2019).

Fig. 7 Right maxilla (GFN-HE 033) of *Zamenis* gr. *longissimus* from Fada Nana Cave in medial view. Scale bar: 1 mm

(Non-snake) Squamata indet.

Material: Right wall: three trunk vertebrae (GFN-HE 0009 and 0123), four caudal vertebrae (GFN-HE 0010-0011), two scapulocoracoids (GFN-HE 0005), 13 humeri (GFN-HE 0006 and 0121), three pelvic girdles (GFN-HE 0122), seven femora (GFN-HE 0007 and 0124), one tibia (GFN-HE 0004). Left wall: one quadrate (GFN-HE 0136), one dentary (GFN-HE 0079), one cervical vertebra (GFN-HE 0108), 17 trunk vertebrae (GFN-HE 0068, 0106), five caudal vertebrae (GFN-HE 0107), two humeri (GFN-HE 0110, 0137), six pelvic girdles (GFN-HE 0135), 38 femora (GFN-HE 0084, 0086), two tibiae (GFN-HE 0085).

Remarks: Lizard remains that are either too poorly preserved or not taxonomically significant are here identified only as indeterminate lizards (i.e. non-snake squamates). For at least some bones, their small size suggests they might belong to the above-described, small-sized lacertid(s).

Serpentes Linnaeus, 1758
Colubroides Zaher et al., 2009
Colubridae Oppel, 1811
Zamenis Wagler, 1830
Zamenis longissimus (Laurenti, 1768)

Zamenis gr. *longissimus*
(Figs. 7, 8a–e)

Material: Right wall: one maxilla (GFN-HE 0033), three precloacal vertebrae (GFN-HE 0133 and 0134). Left wall: seven precloacal vertebrae (GFN-HE 0087 and 0088).

Description

Maxilla: GFN-HE 0033 (Fig. 7) is a 11 mm long, well-preserved right maxilla. It bears 19 tooth positions. Teeth have a relatively similar size (the last ones are slightly smaller than the preceding ones) and, if complete, they display a strongly curved and pointed shape. Located in line with the eighth and ninth tooth positions, the prefrontal process is long and relatively slender. The ectopterygoid process is slightly mediolaterally shorter and anteroposteriorly wider than the prefrontal process; it is in line with the 15^{th}–17^{th} tooth positions. There is no evidence of a diastema preceding the last two tooth positions. In lateral or medial view, the dorsal

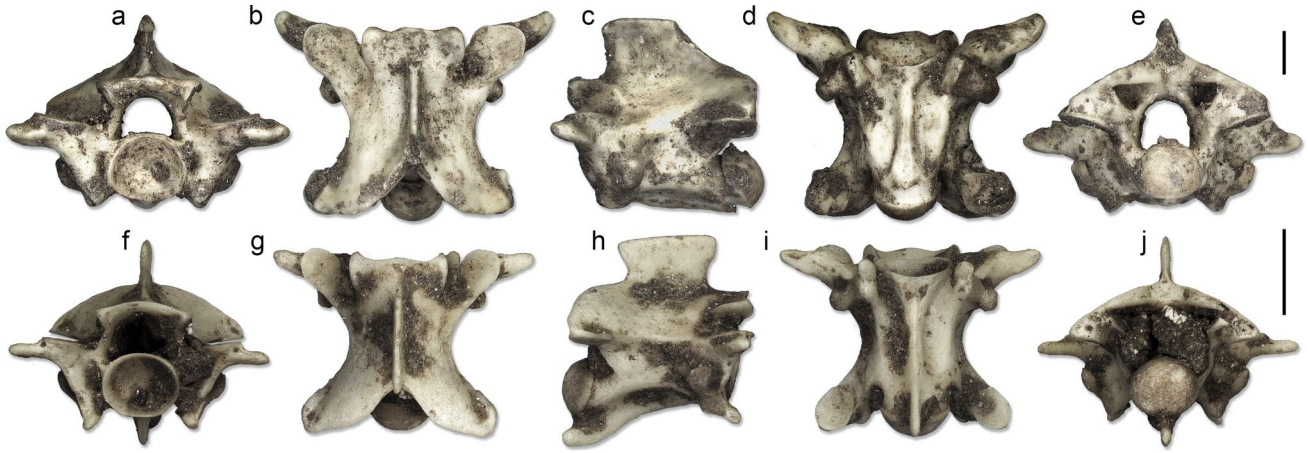

Fig. 8 Vertebrae of colubrids and natricids from Fada Nana Cave. **a–e** precloacal vertebra (GFN-HE 0088) of *Zamenis* gr. *longissimus* in anterior (**a**), dorsal (**b**), left lateral (**c**), ventral (**d**) and posterior (**e**) views. **f–j** precloacal vertebra (GFN-HE 0155) of *Natrix* sp. in anterior (**f**), dorsal (**g**), right lateral (**h**), ventral (**i**) and posterior (**j**) views. Specimens at different magnifications; see corresponding 1 mm scale bars

edge of the maxilla shows a broad, anterior convexity and a modest posterior concavity corresponding to the posterior half of the ectopterygoid process and the area posterior to it.

Precloacal vertebra: These large and robust vertebrae (e.g. Fig. 8a–e) have a procoelous centrum with a distinct hemal keel on the ventral surface. The keel is not flat ventrally and narrow, but tends to enlarge with its posterior end forming a lobe-shaped structure. The neural arch is vaulted in posterior view. The zygosphene typically has a straight anterior margin in dorsal view; however, in GFN-HE 0133 (not figured) this margin is convex. The neural spine is high. The zygapophyses are large, suboval and either subhorizontal or slightly dorsally inclined. The prezygapophyseal accessory processes are well developed, robust (but more slender in GFN-HE 0133) and distally blunt. The parapophyses are only slightly longer than the diapophyses. The largest vertebrae have a centrum length reaching 7 mm.

Remarks: These large-sized colubrid vertebrae can be referred to the *Zamenis longissimus* species complex due to the unflattened and lobe-shaped (= spatulate) hemal keel and the blunt prezygapophyseal processes (Szyndlar 1984, 1991a; Venczel 2000). The species complex includes both *Z. longissimus* and the Italian endemic *Zamenis lineatus*, which cannot be differentiated based on our current knowledge of their vertebral morphology. Only *Z. longissimus* is currently present in the area (Sindaco et al. 2006). Direct comparison of the maxilla GFN-HE 0033 with those of extant *Z. longissimus* (MGPUT MDHC 12, 75, 82, 92, 195, and 309) shows complete size and morphological congruence with that species. Referral to other snake clades currently in the region can be discounted based on morphological criteria. For example, viperids have maxillae strongly reduced and bearing one or few fangs (Zahradnicek et al. 2008; Seghetti et al. 2020; Delfino and Villa 2024), natricids have larger posterior maxillary teeth (Szyndlar and Schleich 1993), and *Hierophis* has a well-developed posterior dorsal notch and diastema (Delfino and Bailon 2000). The relatively large size of the vertebrae and maxilla from Fada Nana Cave also excludes referral to smaller-sized taxa, such as *Coronella*.

Natricidae Bonaparte, 1838
Natrix Laurenti, 1768

Natrix sp.
(Fig. 8f–j)

Material: Left wall: six precloacal vertebrae (GFN-HE 0154 and 0155).

Description

Precloacal vertebra: These precloacal vertebrae (e.g. Fig. 8f–j), the centrum of which never exceeds 4 mm in total length, are elongate and display short and sigmoid hypapophyses. The posterior end of the hypapophysis, where preserved, is rounded. Parapophyseal processes are thin and rounded. The neural arch is vaulted in posterior view and bears a moderately high neural spine. The spine is longer than it is high and overhangs slightly anteriorly and posteriorly in the best-preserved specimens. In dorsal view, the zygosphene has two distinct lateral lobes separated by a relatively straight anterior margin, which shows only a slight anterior convexity. The zygapophyses are slightly inclined dorsally. Prezygapophyseal accessory processes are long, robust, and obtuse distally.

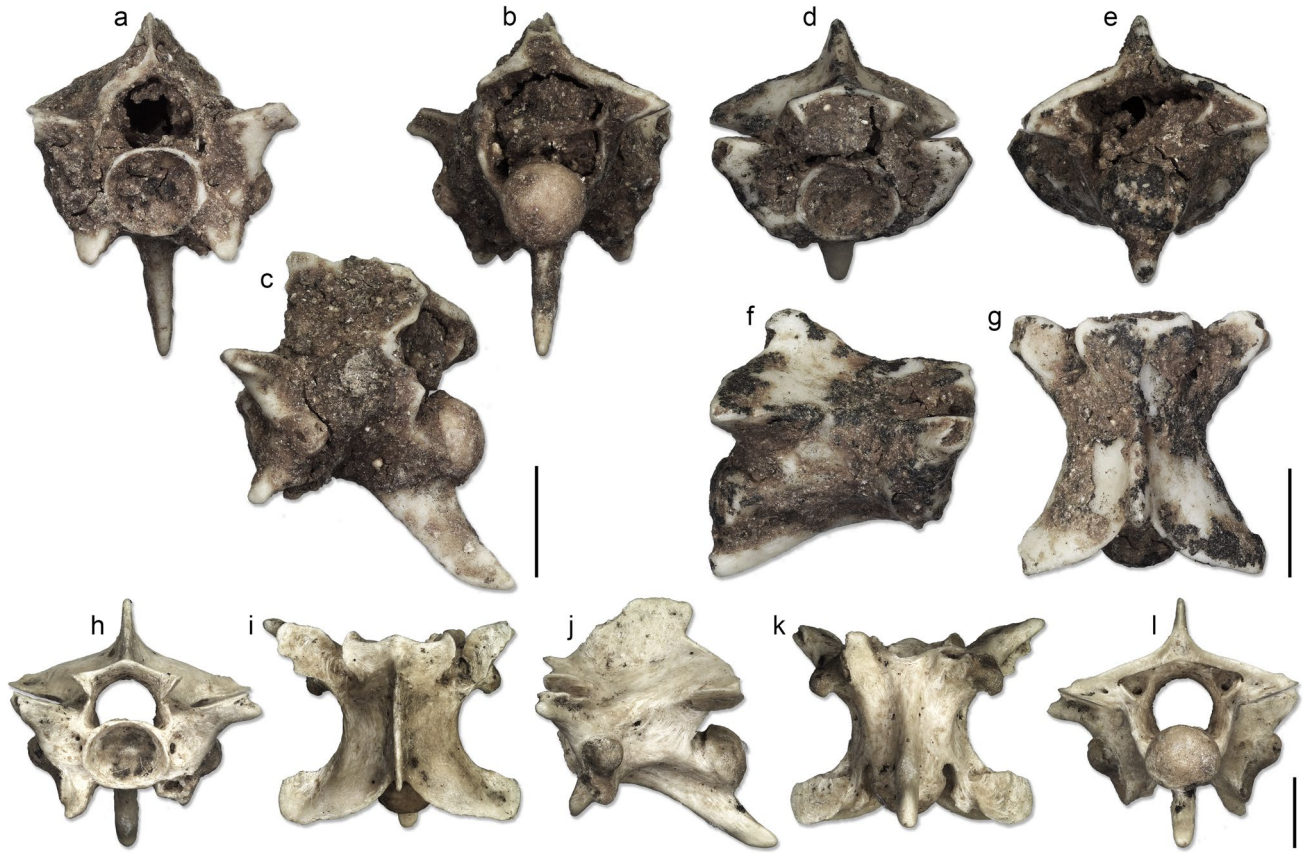

Fig. 9 Vertebrae of *Vipera* gr. *aspis* from Fada Nana Cave. **a**–**c** precloacal vertebra (GFN-HE 0095) in anterior (**a**), posterior (**b**) and left lateral (**c**) views. **d**–**g** precloacal vertebra (GFN-HE 0096) in anterior (**d**), posterior (**e**), right lateral (**f**) and dorsal (**g**) views. **h**–**l** precloacal vertebra (GFN-HE 0113) in anterior (**h**), dorsal (**i**), left lateral (**j**), ventral (**k**) and posterior (**l**) views. Specimens at different magnifications; see corresponding 1 mm scale bars

Remarks: These vertebrae are assigned to *Natrix* based on the vaulted neural arch, moderately high neural spine, sigmoid hypapophysis, and obtuse prezygapophyseal accessory processes (Szyndlar 1984, 1991b). Precloacal vertebrae of *Natrix* are challenging to identify to species, because these bones display a high degree of intracolumnar variation. Characters proposed by Szyndlar (1984) to distinguish *Natrix natrix* from *Natrix tessellata* and *Natrix maura* are problematic because his study relied on limited comparative material (Szyndlar 1991b). A final complication is that *N. natrix* has been recently split (Kindler et al. 2017) with only *Natrix helvetica* currently living in the area (Sindaco et al. 2006). For these reasons, we here leave these vertebrae unassigned to species.

Viperidae Oppel, 1811
Vipera Laurenti, 1768
Vipera aspis (Linnaeus, 1758)

Vipera gr. *aspis*
(Fig. 9)

Material: Right wall: 15 precloacal vertebrae (GFN-HE 0095–0097, 0127, 0128). Left wall: four precloacal vertebrae (GFN-HE 0113–0115)]

Description

Precloacal vertebra: These precloacal vertebrae are elongate and moderately slender. Their procoelous centrum reaches up to 5 mm in length. Ventrally, they have a hypapophysis, which is complete only in GFN-HE 0095 (Fig. 9a–c), 0096 (Fig. 9d–g), 0113 (Fig. 9h–l), 0114, and 0128 (last two not figured). In GFN-HE 0095 and 0113, the hypapophysis is long, straight and distally pointed. GFN-HE 0096, 0114, and 0128 each have a shorter hypapophysis. In posterior view, the neural arch is markedly depressed ("roof-shaped"). The neural spine is always broken. Well-developed and slender parapophyseal processes are preserved in at least some specimens. Where preserved, these processes are short, slender and distally rounded. The zygapophyses are subelliptical and slightly inclined dorsally.

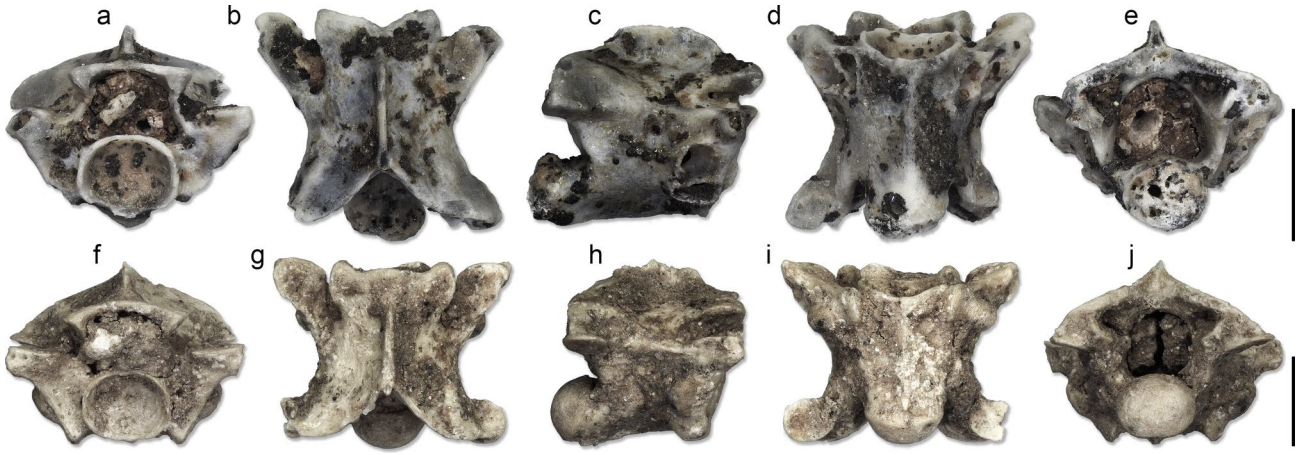

Fig. 10 Vertebrae of Colubroides indeterminate from Fada Nana Cave. **a–e** precloacal vertebra (GFN-HE 0090) in anterior (**a**), dorsal (**b**), right lateral (**c**), ventral (**d**) and posterior (**e**) views. **f–j** precloacal vertebra (GFN-HE 0093) in anterior (**f**), dorsal (**g**), right lateral (**h**), ventral (**i**) and posterior (**j**) views. Specimens at different magnifications; see corresponding 1 mm scale bars

Remarks: Attribution of these vertebrae to a viperid is based on the following features (Szyndlar 1984, 1991b; Venczel 2000): elongate shape; presence of neural spine; long and straight hypapophysis; and "roof-shaped" neural arch. The small size and slender morphology, together with a relatively long hypapophysis and moderate elongation, support assignment to the *Vipera aspis* species complex (Szyndlar 1991b; Bailon et al. 2010). Differences in the development of the hypapophysis are here interpreted as intracolumnar variation, based on personal observations of comparative material at our disposal (MGPUT MDHC specimens). *Vipera aspis* is the only viper currently living in the area (Sindaco et al. 2006).

Colubroides indet.
(Fig. 10)

Material: Right wall: five precloacal vertebrae (GFN-HE 0092–0094). Left wall: one precloacal vertebra (GFN-HE 0090).

Description

Precloacal vertebra: GFN-HE 0090 (Fig. 10a–e) is a small precloacal vertebra, the centrum of which bears an indistinct haemal keel. The keel is narrow and less distinct posteriorly. The neural arch is posteriorly vaulted, but moderately depressed. The paradiapophyses, prezygapophyseal accessory processes, anterior margin of the zygosphene, and neural spine are all broken. The total length of the centrum is roughly 2.5 mm.

The other vertebrae (e.g. Fig. 10f–j) are similar in size to GFN-HE 0090 and similarly poorly preserved. They also have a shallow haemal keel, however, it is more distinct than that of GFN-HE 0090. It is not clear whether this difference is original or due to erosion of the keel in GFN-HE 0090. Also in the other vertebrae their neural arch is vaulted in posterior view, yet not as depressed as in GFN-HE 0090. The zygosphene of these other vertebrae has either a straight or a slightly convex anterior margin. The neural spine is broken in all specimens. Parapophyses and diapophyses are roughly similar in size. The prezygapophyseal accessory processes are either broken off completely or only partially preserved. Where portions are preserved, the prezygapophyseal accessory processes are relatively slender. The vertebrae are relatively short, with a maximum centrum length slightly less than 3.5 mm.

Remarks: These vertebrae share characters of the operative taxon "Colubrines" (sensu Szyndlar 1991a), which is identified by elongate precloacal vertebrae provided with a neural spine and a haemal keel (Szyndlar 1984, 1991a). However, these features are widespread in different branches of the Colubroides clade and, thus, are not useful for identifying these vertebrae to any lower taxonomic level. Based on their small size, these vertebrae are most likely referable to a small-sized snake, as opposed to the larger, above-mentioned colubrid vertebrae referred to the *Zamenis longissimus* species group. Two different morphologies are recognisable based on some minor differences (i.e. the distinctness of the haemal keel and the degree of depression of the neural arch), but it is not possible to determine if these differences indicate the presence of two different species, reflect intracolumnar variation or are preservation artifacts. Deciding among these explanations is hindered by the fact that GFN-HE 0090, the only vertebra that differs in the previously mentioned features, is poorly preserved. Following a cautious approach, we here identify all these vertebrae as belonging to an indeterminate small-sized Colubroides snake.

Table 1 Fossil amphibians, reptiles, and rodents identified from Quaternary deposits in Fada Nana Cave in the present work

		Right wall	Left wall	NISP	MNI
Urodela	*Salamandra salamandra*	x	x	4	2
	Urodela indet.	x		3	2
Anura	*Bufo* gr. *bufo*		x	4	2
	Bufotes gr. *viridis*		x	1	1
	Bufonidae indet.	x	x	21	7
	Rana temporaria	x	x	3	3
	Rana sp.*	x	x	7	5 (+1)
	Ranidae indet.*	x	x	21	4 (+1)
	Anura indet.	x	x	91	6
Squamata	*Lacerta* gr. *viridis*#		x	2	1
	Lacertidae indet.	x	x	82	19
	Anguis gr. *fragilis*	x	x	100	6
	(Non-snake) Squamata indet.	x	x	106	14
	Zamenis gr. *longissimus*	x	x	11	4
	Natrix sp.		x	6	1
	Vipera gr. *aspis*	x	x	19	3
	Colubroides indet.	x	x	6	2
	Serpentes indet.	x	x	36	4
Rodentia	*Arvicola mosbachensis*	x	x	13	7
	Dinaromys cf. *bogdanovi*	x	x	53	21
	Microtus (*Terricola*) *arvalidens*	x		86	-
	Pliomys coronensis	x		4	3
	Pliomys episcopalis	x		33	17
	Cricetulus bursae	x	x	9	5
	Glis glis	x	x	6	2

Taxa marked with * (*Rana* sp. and Ranidae indet.) are present both in the Middle Pleistocene assemblage and in the Recent assemblage, whereas the taxon marked with # (*Lacerta* gr. *viridis*) was identified only in the Recent assemblage. For *Rana* sp. and Ranidae indet., MNI for the Recent assemblage is reported between parentheses. Number of individuals was not estimated for *Microtus* (*Terricola*) *arvalidens*, because relevant data was not recorded on site. Abbreviations: *MNI*, minimum number of individuals; *NISP*, number of identifiable specimens.

Serpentes indet.

Material: Right wall: six anterior trunk vertebrae (GFN-HE 0036), two precloacal vertebrae (GFN-HE 0117), four vertebral fragments (GFN-HE 0035), four ribs (GFN-HE 0034 and 0118). Left wall: nine precloacal vertebrae (GFN-HE 0089), 11 ribs (GFN-HE 0091 and 0109).
Remarks: These fossils pertain to snakes, but they are either too poorly preserved or too diagnostically uninformative to be identified more precisely.

Discussion

The Middle Pleistocene palaeoenviroment surrounding Fada Nana Cave

Due to their strict environmental sensitivity, amphibians and reptiles are often used as proxies to reconstruct palaeoclimate and palaeoenvironment near the localities where their fossils are found (e.g. Böhme 2003; Böhme et al. 2006, 2008; Blain et al. 2008, 2009, 2018, 2019; Agustí et al. 2009; Bañuls Cardona et al. 2012; López-García et al. 2014; Villa et al. 2018b; Georgalis et al. 2019; Cruz et al. 2021). This was done recently with Early Pleistocene (Villa et al. 2018a, 2020a) and Holocene (Villa et al. 2020b) herpetofaunas from Veneto, and the new assemblage herein reported offers the opportunity to make similar inferences for the Middle Pleistocene in the same region. Habitat requirements used to make such inferences (see below) are mostly based on data for extant species provided by Lanza et al. (2007), Corti et al. (2011), Speybroeck et al. (2016), and Di Nicola et al. (2019). As explained earlier in the "Geological and chronological setting" section, right and left walls only indicate locations of specimens within the cave. Excluding the Recent bones (i.e. *Rana* sp. squamosal, Ranidae indet. parasphenoid, and *Lacerta* gr. *viridis* frontal and compound bone), the fossils make up a coherent assemblage dating to

the Middle Pleistocene. Because of this, the Middle Pleistocene fauna is herein interpreted as a whole, for the scope of the following palaeoenvironmental inferences.

The identification of several amphibian taxa as well as the grass snake *Natrix* supports the presence of nearby water bodies. The low abundance of fossils pertaining to species most directly tied with water suggests that the cave entrance was likely not in close proximity to the latter. Nevertheless, the availability of at least temporary water bodies in the area is confidently assumed, thanks to the identification of grass snakes, brown frogs (genus *Rana*), and, above all, green toads (*Bufotes* gr. *viridis*). Streams with well oxygenated waters where larvae of fire salamanders could develop were potentially also present. A number of species, including in particular the fire salamander and the Aesculapian snake *Zamenis* gr. *longissimus*, are indicative of a forested environment. More generalist species, such as the common frog *Rana temporaria* and the slow worm *Anguis* gr. *fragilis*, are also often found in woodlands or meadows and clearings associated with woodlands. When considering the Minimum Number of Individuals (MNI; Table 1), amphibian and reptile species or species groups associated or potentially associated with forested areas make up 62.5% (15 individuals = four *S. salamandra*, three *R. temporaria*, six *Anguis* gr. *fragilis*, and four *Zamenis* gr. *longissimus*) of the taxa identified at genus rank or lower (i.e. components of the assemblage more suitable for quantitative palaeoecological interpretations; total MNI = 24). More open, ecotonal environments can be also inferred, based on the green toads and especially the reptiles, the latter of which could bask there. Furthermore, vipers (genus *Vipera*) favour areas with rocks where they can bask and hide. In summary, the identified amphibian and reptile species allow us to reconstruct a moist and ecotonal environment during the Middle Pleistocene for the area surrounding Fada Nana Cave, with water bodies (some of which were temporary), a significant tree coverage (but likely not a dense and closed forest), and patches of open meadows.

This reconstruction is also supported by the composition of the micromammal assemblage. The occurrence of *Arvicola* confirms the presence of water-related environments (e.g. streams and ponds) in the vicinity of the site. Whereas *Clethrionomys glareolus*, *Apodemus* sp., *Glis glis*, and *Sciurus vulgaris* are generally associated with mature woodland and shrublands, *Dinaromys* and *Marmota* prefer open areas with exposed rocky substrate (IUCN 2024; Wilson et al. 2017). Species in the *Microtus* group favour open habitats, like meadows and grasslands (Wilson et al. 2017), completing the mosaic-like picture of the landscape surrounding Fada Nana Cave. Our reconstruction further matches indications given by pollen data for the Middle Pleistocene in northern Italy, where interglacials are characterised by a dominance of deciduous forests and with a significant expansion of steppes and grasslands only during glacial phases (Bertini 2010; Combourieu-Nebout et al. 2015; Strani et al. 2021; Bertini and Combourieu-Nebout 2023). It also agrees with a referral of the assemblage to an interglacial stage characterised by significant forest development, such as MIS 13, as recognised in other subregions of Mediterranean Europe (e.g. Iberia: Oliveira et al. 2020; Balkans: Tzedakis et al. 2006) and in central and southern Italy (Russo Ermolli et al. 2015; Margari et al. 2018).

The reconstructed palaeoenvironment around Fada Nana Cave is like those inferred from amphibians and reptiles recovered in two older, Early Pleistocene-age sites located nearby in northern Verona province, namely Rivoli Veronese (Gelasian: Villa et al. 2018a) and Monte La Mesa (Calabrian: Villa et al. 2020a). Such similarity may indicate a certain environmental continuity in this region during the Early–Middle Pleistocene, even though we must acknowledge that at least Rivoli Veronese marks a cool, potentially glacial phase and that we have no data on other Middle Pleistocene local glacial assemblages to compare with. Additional data on other Pleistocene sites and faunas from Verona province are needed to further investigate and test this possibility.

Fada Nana Cave and the relictual *Pseudopus* population in the Quaternary of Veneto

The palaeoherpetological assemblage herein described from the Middle Pleistocene deposits of Fada Nana Cave (Table 1) includes species commonly recognised in other Quaternary localities within the Veneto region (Delfino et al. 2008; Villa et al. 2020a), among which bufonids, ranids, small lacertids, the slow worm, and the three different snakes we were able to identify. In addition to these, notable findings worth emphasising are the fire salamander, *Salamandra salamandra*, and the common frog, *Rana temporaria*. For both species, these are the oldest occurrences known to date for Italy (Bartolini et al. 2014; Macaluso et al. 2022), with only still unpublished material from the nearby locality of Valdiporro potentially being of comparable age (Delfino 2002; Bartolini et al. 2014; M.D., pers. obs.). Comparisons between Fada Nana Cave with other Quaternary localities in Veneto (see Delfino et al. 2008; Villa et al. 2018a, 2020a, b) reveal some intriguing absences. The absence at Fada Nana Cave of certain taxa (e.g. pleurodeline newts, fire-bellied toads, tree frogs, and smooth snakes) might be simply explained by their overall rarity in the fossil record, whereas others (i.e. allocaudates and plethodontid newts) likely disappeared long before the end of the Early Pleistocene (Villa et al. 2021). There is one taxon, however, whose absence from the Fada Nana Cave assemblage is more puzzling: the anguid *Pseudopus*.

In the Quaternary of Veneto, this large-sized lizard genus is reported from localities both older and younger than Fada Nana Cave. The oldest record is a tentative occurrence (cf. *Pseudopus* sp.) from the Gelasian of Rivoli Veronese, based on a few, badly preserved bones described by Villa et al. (2018a). Subsequently, Villa et al. (2020a) reported a large number of cranial and postcranial bones, from the Biharian of Monte La Mesa, which they tentatively referred to *Pseudopus* cf. *pannonicus*. This attribution can be now corroborated after the revised diagnosis of *P. pannonicus* recently provided by Loréal et al. (2024). Adding to the characters mentioned by Villa et al. (2020a), the fossils from Monte La Mesa can be confidently referred to this species based on: 1) their distinctly large size (comparable with the Hungarian type material, redescribed by Loréal et al. 2024); 2) absence of permanently fused teeth in the posterior section of both the maxillary and dentary tooth rows (see also Roček 1980, 2019); and 3) presacral vertebrae more robust and less elongate than in *Pseudopus apodus*. Additional occurrences of an indeterminate *Pseudopus* species were preliminary reported, but neither described nor figured, by Delfino et al. (2008; see also Villa et al. 2020a: table 2) from the earliest Middle Pleistocene of Zoppega 2, the Middle Pleistocene of Viatelle, and the Late Pleistocene of Grotta della Volpe. All these localities with *Pseudopus* remains are in Verona province, relatively close to one another and to Fada Nana Cave. They also testify to the persistence of *Pseudopus* in the area at least from the Early to the Late Pleistocene. The question arises, then, why is this large lizard not found in Fada Nana Cave?

A potential explanation might be found in the different elevations of the sites. Viatelle and Zoppega 2 are part of a complex of karst fillings called "Brecce di Soave" (near the homonymous village of Soave), which is currently placed at an altitude of about 70 m asl according to Bartolomei (1970). More precisely, Zoppega 2 and Viatelle open at 70 and 80 m asl, respectively (elevations retrieved from the Catasto Grotte Veneto website). The elevation of the Rivoli Veronese fossiliferous fissure is 190 m asl (Berto et al. 2022), whereas the palaeontological sites of Monte La Mesa and Grotta della Volpe are both located at 200 m asl (Marchetti et al. 2000; Berto 2012). All these sites are at far lower altitudes than Fada Nana Cave, which opens at 751 m asl (elevation retrieved from the Catasto Grotte Veneto website) on a steep slope. Because of the absence of tectonic events in the Quaternary that may have moved the relative position of the sites, the same significant relative altitude difference most likely stayed constant throughout glacial/interglacial phases in the Pleistocene, despite variation in the northern Adriatic Sea level. Altitude was reported as one of the most important variables explaining the distribution of the extant *Pseudopus apodus* in Iran by Nasrabadi et al. (2018a). Baran et al. (1988) reported two ecotypes within the species: western Turkish and European populations are linked to coastal areas, whereas Asian populations also inhabit higher elevations. In agreement with this framework, the distribution of *P. apodus* ranges from 600 to 1000 m asl in Jordan (Rifai et al. 2005) versus mostly below 400 m asl in Europe (Speybroeck et al. 2016; but note that isolated populations reaching up to 800 m asl in Bulgaria were mentioned by Telenchev et al. 2015, citing Stojanov et al. 2011). Nasrabadi et al. (2018b) wrote that currently suitable areas for the species are to be found in plains and valleys. According to those authors' models of the effects of anthropogenic climate change, by 2070 suitable areas for *P. apodus* are projected to move towards mountainous areas because of decreasing precipitation in lowlands. An opposite trend may be hypothesised for Quaternary populations of *Pseudopus* in northern Italy, with the animals even more tied to lower altitudes in the cooler Pleistocene climate. This would explain their absence in the Middle Pleistocene Fada Nana assemblage. However, more data are needed to confirm that explanation. In particular, more information on altitudinal ranges for localities containing the extinct *P. pannonicus*, whose presence is confirmed at least during the Early Pleistocene in the area, could test this and the suggestion by Klembara et al. (2010) that *P. pannonicus* tolerated wider ecological requirements than *P. apodus*. A deeper (palaeo) biological comparison between the extant *P. apodus* and extinct *Pseudopus* species to evaluate potential similarities or differences in their preferred habitats is also desirable. In any case, suitable conditions for *Pseudopus* in northeastern Italy started decreasing during the Last Interglacial, and ultimately disappeared with the onset of the Last Glacial Maximum (Macaluso et al. 2023a: fig. 4).

Conclusions

Thanks to our study of the micromammal assemblage (*Arvicola mosbachensis*, *Dinaromys* cf. *bogdanovi*, *Microtus* (*Terricola*) *arvalidens*, *Pliomys coronensis*, *Pliomys episcopalis*, *Cricetulus bursae*, and *Glis glis*) associated with the herpetofaunal remains, and in agreement with other mammals previously reported from Fada Nana Cave, we tentatively assign this Middle Pleistocene fauna to either the MIS 13 or 15 Interglacial, within the early Torigian. Amphibians and reptiles from the cave (Table 1) represent a moderately diversified palaeoherpetofauna. Identified amphibian taxa include one urodele (*Salamandra salamandra*) and at least three anurans (*Bufo* gr. *bufo*, *Bufotes* gr. *viridis*, and *Rana temporaria*, plus other remains assigned less precisely to bufonids and ranids that may or may not pertain to the same taxa). Lizards are represented by *Anguis* gr. *fragilis* and one or more small lacertids (previously preliminary referred to cf. *Podarcis*

sp. by Delfino et al. 2008), whose precise identification is left as indeterminate for the time being. Indeterminate lizard remains are also present. Absence of the glass lizard *Pseudopus* is intriguing, given its presence in other nearby sites spanning the Pleistocene; a possible explanation is the significantly higher elevation of Fada Nana Cave, based on comparisons with the reported ecological requirements of extant *P. apodus*, but this hypothesis needs to be further investigated. Snakes are comprised of *Zamenis* gr. *longissimus*, *Natrix* sp., *Vipera* gr. *aspis*, potentially an indeterminate additional small Colubroides, and indeterminate snake fossils. Report of the Western whip snake *Hierophis viridiflavus* by Villa et al. (2020a: table 2) was a mistake, and is corrected here. A few fossils coming from Recent (archaeological) deposits within the cave pertain to a green lizard, *Lacerta* gr. *viridis*, and additional ranids, mainly attributed to brown frogs, *Rana* sp. The Middle Pleistocene faunal assemblage of amphibians, reptiles and micro-mammals suggests a forested and moist environment for the area surrounding Fada Nana Cave when the fossils were deposited, with the close presence of (at least temporary) water bodies and open meadows in an ecotonal context.

Supplementary Information The online version contains supplementary material available at https://doi.org/10.1007/s12549-025-00662-5.

Acknowledgements This paper is dedicated to Marton Venczel for his inspiring contribution to the field of palaeoherpetology. Prof. Benedetto Sala is thanked for having involved the senior author in the 2004 excavations at Fada Nana Cave and for having entrusted us with the study of the materials here described, as well as for providing his support and his valuable comments and suggestions on micromammal identification. Prof. Sala and Ugo Sauro further provided us with the original picture of Fada Nana Cave used for Fig. 1c. We also thank Loredana Macaluso for discussions on the urodele identifications and Sara Monti for taking some of the photographs of the anuran remains. Editorial handling and suggestions by editor-in-chief Dieter Uhl, managing editor Sinje Weber, and associate and guest editor Jim Gardner, as well as comments by the two reviewers, Alfred Lemierre and Hugues-Alexandre Blain, are greatly appreciated. This is publication number 382 of the Museo di Geologia e Paleontologia collections at the Università degli Studi di Torino.

Author contributions All authors took part in the conceptualization, funding acquisition, investigation, and visualization of the work presented in this article. Massimo Delfino supervised the study. Andrea Villa and Elisa Luzi prepared the original draft, and all authors reviewed and edited the final version of the article.

Funding Open Access funding provided thanks to the CRUE-CSIC agreement with Springer Nature. AV is funded by the Secretaria d'Universitats i Recerca of the Departament de Recerca i Universitats, Generalitat de Catalunya, through a Beatriu de Pinós postdoctoral grant (2021 BP 00038). He further acknowledges support by the Agència de Gestió d'Ajuts Universitaris i de Recerca of the Generalitat de Catalunya (consolidated research group"Neogene and Quaternary Vertebrate Paleobiodiversity (NQVP)", 2021 SGR 00620), the Agencia Estatal de Investigación of the Spanish Ministerio de Ciencia e Innovación (MCIN/AEI/https://doi.org/10.13039/501100011033/) (R+D+I project PID2020-117289GB-I00), and the CERCA Programme/Generalitat de Catalunya.

Data availability All data generated or analysed during this study are included in this article. All fossils are stored in the collections of the Dipartimento di Biologia ed Evoluzione, Università degli Studi di Ferrara, Italy.

Declarations

Conflict of interest The authors declare they have no known conflict of interest related to this study.

Open Access This article is licensed under a Creative Commons Attribution 4.0 International License, which permits use, sharing, adaptation, distribution and reproduction in any medium or format, as long as you give appropriate credit to the original author(s) and the source, provide a link to the Creative Commons licence, and indicate if changes were made. The images or other third party material in this article are included in the article's Creative Commons licence, unless indicated otherwise in a credit line to the material. If material is not included in the article's Creative Commons licence and your intended use is not permitted by statutory regulation or exceeds the permitted use, you will need to obtain permission directly from the copyright holder. To view a copy of this licence, visit http://creativecommons.org/licenses/by/4.0/.

References

Abbazzi, L., Fanfani, F., Ferretti, M. P., Rook, L., Cattani, L., Masini, F., Mallegni, F., Negrino, F., & Tozzi, C. (2000). New human remains of archaic *Homo sapiens* and lower palaeolithic industries from Visogliano (Duino Aurisina, Trieste, Italy). *Journal of Archaeological Science, 27*(12), 1173–1186.

Agustí, J., Blain, H.-A., Cuenca-Bescòs, G., & Bailon, S. (2009). Climate forcing of first hominid dispersal in Western Europe. *Journal of Human Evolution, 57*(6), 815–821.

Auffenberg, W. (1963). The fossil snakes of Florida. *Tulane Studies in Zoology, 10*(3), 131–216.

Bailon, S. (1999). Différenciation ostéologique des anoures (Amphibia, Anura) de France. In J. Desse & N. Desse-Berset N. (Eds.), *Fiches d'ostéologie animale pour l'Archéologie,* (Série C: Varia, 1, pp. 1–41). Antibes: APdCA.

Bailon, S., Bover, P., Quintana, J., & Alcover, J. A. (2010). First fossil record of *Vipera* laurenti 1768 "oriental vipers complex" (Serpentes: Viperidae) from the Early Pliocene of the western Mediterranean islands. *Comptes Rendus Palevol, 9*(4), 147–154.

Bañuls Cardona, S., López-García, J. M., Blain, H.-A., & Canals Salomó, A. (2012). Climate and landscape during the Last Glacial Maximum in southwestern Iberia: The small-vertebrate association from the Sala de las Chimeneas, Maltravieso, Extremadura. *Comptes Rendus Palevol, 11*(1), 31–40.

Barahona, F., & Barbadillo, L. J. (1997). Identification of some Iberian lacertids using skull characters. *Revista Española de Herpetología, 11,* 47–62.

Barahona, F., & Barbadillo, L. J. (1998). Inter- and intraspecific variation in the post-natal skull of some lacertid lizards. *Journal of Zoology, 245*(4), 393–405.

Baran, İ., Kasparek, M., & Öz, M. (1988). On the distribution of the Slow Worm, *Anguis fragilis*, and the European Glass Lizard, *Ophisaurus apodus*, in Turkey. *Zoology in the Middle East, 2*(1), 57–62.

Bartolini, S., Cioppi, E., Rook, L., & Delfino, M. (2014). Late Pleistocene fossils and the future distribution of *Rana temporaria* (Amphibia, Anura) along the Apennine Peninsula (Italy). *Zoological Studies, 53,* 76.

Bartolomei, G. (1970). Primi contributi alla conoscenza del *Dolomys* pleistocenici del Veneto e del Carso. *Memorie del Museo Civico di Storia Naturale di Verona, 17,* 79–139.

Batsch, A. J. G. C. (1796). *Umriß der gesammten Naturgeschichte: ein Auszug aus den frühern Handbüchern des Verfassers für seine Vorlesungen.* Jena and Leipzig: Christian Ernst Gabler.

Bertini, A. (2010). Pliocene to Pleistocene palynoflora and vegetation in Italy: state of the art. *Quaternary International, 225*(1), 5–24.

Bertini, A., & Combourieu-Nebout, N. (2023). Piacenzian to late Pleistocene flora and vegetation in Italy: a moving sketch. *Alpine and Mediterranean Quaternary, 36*(1), 91–119.

Berto, C. (2012). *Distribuzione ed evoluzione delle associazioni a piccoli mammiferi nella penisola italiana durante il Pleistocene superiore.* Unpublished PhD thesis, Università degli Studi di Ferrara.

Berto, C., Luzi, E., Marchetti, M., Pereswiet-Soltan, A., & Sala, B. (2022). Faunal renewals during the Early Pleistocene on the northern Italian Peninsula: Climate and environment reconstructions inferred from the Rivoli Veronese small mammal assemblage (Adige River valley, Verona, Italy). *Quaternary International, 633,* 134–153.

Blain, H. B., & Arribas, O. J. (2017). A description of the skeletal morphology of *Rana pyrenaica* (Anura: ranidae), with comments on functional morphology, ecological adaptation and relationships with other Iberian ranids. *Zootaxa, 4319*(3), 510–530.

Blain, H.-A., Bailon, S., & Cuenca-Bescós, G. (2008). The Early–Middle Pleistocene palaeoenvironmental change based on the squamate reptile and amphibian proxies at the Gran Dolina site, Atapuerca, Spain. *Palaeogeography, Palaeoclimatology, Palaeoecology, 261*(1–2), 177–192.

Blain, H.-A., Bailon, S., Cuenca-Bescós, G., Arsuaga, J. L., Bermúdez de Castro, J. M., & Carbonell, E. (2009). Long-term climate record inferred from early-middle Pleistocene amphibian and squamate reptile assemblages at the Gran Dolina Cave, Atapuerca, Spain. *Journal of Human Evolution, 56*(1), 55–65.

Blain, H.-A., Delfino, M., Berto, C., & Arzarello, M. (2016). First record of *Pelobates syriacus* (Anura, Amphibia) in the early Pleistocene of Italy. In J. D. Gardner &, T. Přikryl (Eds.), *Contributions in honour of Zbyněk Roček. Palaeobiodiversity and Palaeoenviroments, 96*(1), 111–124.

Blain, H.-A., Cruz Silva, J. A., Jiménez Arenas, J. M., Margari, V., & Roucoux, K. (2018). Towards a Middle Pleistocene terrestrial climate reconstruction based on herpetofaunal assemblages from the Iberian Peninsula: state of the art and perspectives. *Quaternary Science Reviews, 191,* 167–188.

Blain, H.-A., Fagoaga, A., Ruiz-Sánchez, F. J., Bisbal-Chinesta, J. F., & Delfino, M. (2019). Latest Villafranchian climate and landscape reconstructions at Pirro Nord (southern Italy). *Geology, 47*(9), 829–832.

Blainville, H. de (1816). Prodrome d'une nouvelle distribution systématique du règne animal. *Bulletin des Sciences de la Société philomatique de Paris, Juillet 1816,* '105–112' [113–120] + 121–124.

Böhme, M. (2003). The Miocene Climatic Optimum: evidence from ectothermic vertebrates of Central Europe. *Palaeogeography, Palaeoclimatology, Palaeoecology, 195*(3–4), 389–401.

Böhme, M., Ilg, A., Ossig, A., & Küchenhoff, H. (2006). New method to estimate paleoprecipitation using fossil amphibians and reptiles and the middle and late Miocene precipitation gradients in Europe. *Geology, 34*(6), 425–428.

Böhme, M., Ilg, A., & Winklhofer, M. (2008). Late Miocene "washhouse" climate in Europe. *Earth and Planetary Science Letters, 275*(3–4), 393–401.

Bona, F., Bellucci, L., Casali, D., Schirolli, P., & Sardella, R. (2016). *Macaca sylvanus* Linnaeus 1758 from the Middle Pleistocene of Quecchia quarry (Brescia, Northern Italy). *Hystrix, Italian Journal of Mammalogy, 27*(2), 158–162.

Bonaparte, C. L. J. L. (1838). *Iconographia della fauna italica per le quattro classi degli animali vertebrati. Tomo II. Amphibi. Fascicolo 22.* Roma: Salviucci.

Čerňanský, A. (2010). Earliest world record of green lizards (Lacertilia, Lacertidae) from the Lower Miocene of Central Europe. *Biologia, 65,* 737–741.

Čerňanský, A. (2025). Green lizards (Squamata, Lacertidae) from ?Pliocene deposits of Węże I in southern Poland, with comments on cranial features for selected lacertids. In J. D. Gardner, & Z. Szentesi (Eds.), *Festschrift for Márton Venczel. Palaeobiodiversity and Palaeoenvironments 105*(2). https://doi.org/10.1007/s12549-024-00619-0. [this issue]

Čerňanský, A., & Syromyatnikova, E. V. (2019). The first Miocene fossils of *Lacerta* cf. *trilineata* (Squamata, Lacertidae) with a comparative study of the main cranial osteological differences in green lizards and their relatives. *PLoS ONE, 14*(8), e0216191.

Čerňanský, A., Yaryhin, O., Ciceková, J., Werneburg, I., Hain, M., & Klembara, J. (2019). Vertebral comparative anatomy and morphological differences in anguine lizards with a special reference to *Pseudopus apodus*. *The Anatomical Record, 302*(2), 232–257.

Collareta, A., Casati, S., Zuffi, M. A. L., & Di Cencio, A. (2020). First authentic record of the freshwater turtle *Mauremys* from the Upper Pliocene of Italy, with a new occurrence of the rarely reported ichnotaxon *Thatchtelithichnus holmani*. *Carnets de Gèologie, 20*(16), 301–313.

Combourieu-Nebout, N., Bertini, A., Russo-Ermolli, E., Peyron, O., Klotz, S., Montade, V., Fauquette, S., Allen, J., Fusco, F., Goring, S., Huntley, B., Joannin, S., Lebreton, V., Magri, D., Orain, R., & Sadori, L. (2015). Climate changes in the central Mediterranean and Italian vegetation dynamics since the Pliocene. *Review of Palaeobotany and Palynology, 218,* 127–147.

Corti, C., Capula, M., Luiselli, L., Razzetti, E., & Sindaco, R. (2011). *Fauna d'Italia, Vol. XLV, Reptilia.* Bologna: Calderini.

Cruz, J. A., Alarcón-D, I., Figueroa-Castro, D. M., & Castañeda-Posadas, C. (2021). Fossil pigmy rattlesnake inside the mandible of an American mastodon and use of fossil reptiles for the paleoclimatic reconstruction of a Pleistocene locality in Puebla, Mexico. *Quaternary International, 574,* 116–126.

Dalla Valle, C. (2011). *I micromammiferi del Toringiano inferiore dei tagli dal 37 al 29 del Riparo di Visogliano (Duino Aurisina, Trieste).* Unpublished MSc thesis, Università degli Studi di Ferrara.

Daoud, A. (1993). Evolution of Gliridae (Rodentia, Mammalia) in the Pliocene and Quaternary of Poland. *Acta Zoologica Cracoviensia, 36*(2), 199–231.

Delfino, M. (2002). *Erpetofaune italiane del Neogene e del Quaternario.* Unpublished PhD Thesis, Università degli Studi di Modena e Reggio Emilia.

Delfino, M. (2003). A Pleistocene amphisbaenian from Sicily. *Amphibia-Reptilia, 24*(4), 407–414.

Delfino, M., & Bailon, S. (2000). Early Pleistocene herpetofauna from Cava Dell'Erba and Cava Pirro (Apulia, Southern Italy). *The Herpetological Journal, 10*(3), 95–110.

Delfino, M., & Sala, B. (2007). Late Pliocene Albanerpetontidae (Lissamphibia) from Italy. *Journal of Vertebrate Paleontology, 27*(3), 716–719.

Delfino, M., & Villa, A. (2024). An overview of the skeleton of reptiles. In U. Joger (Ed.), *Handbook of Zoology, Reptilia, Volume 1: General Biology, Archosauria, Chelonia* (pp. 39–56). Berlin/Boston: Walter de Gruyter GmbH.

Delfino, M., Bacciotti, M., Bon, M., Pitruzzella, G., Sala, B., & Rook, L. (2008). A general overview on the Plio-Quaternary herpetofauna of Veneto. In *Herpetologia Sardiniae* (pp. 196–199). Latina: Societas Herpetologica Italica/Edizioni Belvedere.

Delfino, M., Bailon, S., & Pitruzzella, G. (2011). The late Pliocene amphibians and reptiles from "Capo Mannu D1 local fauna" (Mandriola, Sardinia, Italy). *Geodiversitas, 33*(2), 357–382.

Di Nicola, M. R., Cavigioli, L., Luiselli, L., & Andreone, F. (2019). *Anfibi & rettili d'Italia.* Latina: Edizioni Belvedere.

Duméril, A. M. C. (1805). *Zoologie Analytique, ou Méthode Naturelle de Classification des Animaux, Rendue plus Facile à l'Aide de Tableaux Synoptiques.* Paris: Allais.

Falguères, C., Bahain, J. J., Tozzi, C., Boschian, G., Dolo, J. M., Mercier, N., Valladas, H., & Yokoyama, Y. (2008). ESR/U-series chronology of the Lower Palaeolithic palaeoanthropological site of Visogliano, Trieste, Italy. *Quaternary Geochronology, 3*(4), 390–398.

Fauquette, S., & Bertini, A. (2003). Quantification of the northern Italy Pliocene climate from pollen data: evidence for a very peculiar climate pattern. *Boreas, 32*(2), 361–369.

Garsault, F. A. P. de. (1764). *Les figures des plantes et animaux d'usage en médecine, décrits dans la matière médicale de Mr. Geoffroy Médecin, dessinés d'après nature. Niquet scrip. [Tome 5].* Paris: Mrs. Defehrt, Prevost, Duflos, Martinet & co.

Georgalis, G. L., Villa, A., Ivanov, M., Vasilyan, D., & Delfino, M. (2019). Fossil amphibians and reptiles from the Neogene locality of Maramena (Greece), the most diverse European herpetofauna at the Miocene/Pliocene transition boundary. *Palaeontologia Electronica, 22.3.68,* 1–99.

Gleed-Owen, C. P. (1998). *Quaternary herpetofaunas of the British Isles: taxonomic descriptions, palaeoenvironmental reconstructions, and biostratigraphic implications.* Unpublished PhD Thesis, Coventry University.

Goldfuss, G. A. (1820). *Handbuch der Zoologie.* Nuremberg: J. L. Schrag.

Gómez, R. O., & Turazzini, G. F. (2016). An overview of the ilium of anurans (Lissamphibia, Salientia), with a critical appraisal of the terminology and primary homology of main ilial features. *Journal of Vertebrate Paleontology, 36*(1), e1030023.

Gray, J. E. (1825). A synopsis of the genera of reptiles and Amphibia, with a description of some new species. *Annals of Philosophy, new series, 10*, 193–217.

Gvoždík, V., Jandzik, D., Lymberakis, P., Jablonski, D., & Moravec, J. (2010). Slow worm, *Anguis fragilis* (Reptilia: Anguidae) as a species complex: Genetic structure reveals deep divergences. *Molecular Phylogenetics and Evolution, 55*(2), 460–472.

Gvoždík, V., Benkovský, N., Crottini, A., Bellati, A., Moravec, J., Romano, A., Sacchi, R., & Jandzik, D. (2013). An ancient lineage of slow worms, genus *Anguis* (Squamata: Anguidae), survived in the Italian Peninsula. *Molecular Phylogenetics and Evolution, 69*(3), 1077–1092.

Haller-Probst, M., & Schleich, H. H. (1994). Vergleichende osteologische Untersuchungen an einigen Urodelen Eurasiens (Amphibia; Urodela, Salamandridae, Proteidae). *Courier Forschungsinstitut Senckenberg, 173*, 23–77.

Heinrich, W.-D. (1978). Zur biometrischen Erfassung eines Evolutionstrends bei *Arvicola* (Rodentia, Mammalia) aus dem Pleistozän Thüringens. *Säugetierkundliche Informationen*, *2*, 3–21.

Hewitt, G. M. (1996). Some genetic consequences of ice ages, and their role in divergence and speciation. *Biological Journal of the Linnean Society, 58*(3), 247–276.

Hewitt, G. M. (1999). Post-glacial re-colonization of European biota. *Biological Journal of the Linnean Society, 68*(1–2), 87–112.

Hewitt, G. (2000). The genetic legacy of the Quaternary ice ages. *Nature, 405,* 907–913.

Hír, J. (1998). Cricetids (Rodentia, Mammalia) of the Early Pleistocene vertebrate fauna of Sommsich-hegy 2 (Southern Hungary, Villány Mountains). *Annales Historico-Naturales Musei Nationalis Hungarici, 90,* 57–89.

Holman, J.A. (1998). *Pleistocene amphibians and reptiles in Britain and Europe.* New York/Oxford: Oxford University Press.

IUCN (2024). *The IUCN Red List of Threatened Species. Version 2024-2*. International Union for Conservation of Nature and Natural Resources. Retrieved December 30th, 2024 from https://www.iucnredlist.org

Kindler, C., Chèvre, M., Ursenbacher, S., Böhme, W., Hille, A., Jablonski, D., Vamberger, M., & Fritz, U. (2017). Hybridization patterns in two contact zones of grass snakes reveal a new Central European snake species. *Scientific Reports, 7,* 7378.

Klembara, J. (1981). Beiträg zur Kenntnis der Subfamilie Anguinae (Reptilia, Anguidae). *Acta Universitatis Carolinae, Geologica, 2*, 121–168.

Klembara, J., Böhme, M., & Rummel, M. (2010). Revision of the anguine lizard *Pseudopus laurillardi* (Squamata, Anguidae) from the Miocene of Europe, with comments on paleoecology. *Journal of Paleontology, 84*(2), 159–196.

Klembara, J., Hain, M., & Dobiašová, K. (2014). Comparative anatomy of the lower jaw and dentition of *Pseudopus apodus* and the interrelationships of species of subfamily Anguinae (Anguimorpha, Anguidae). *The Anatomical Record, 297*(3), 516–544.

Lanza, B. & Corti, C. (1996). Evolution of knowledge on the Italian herpetofauna during the 20th century. *Bollettino del Museo civico di Storia Naturale di Verona, 20,* 373–436.

Lanza, B., Andreone, F., Bologna, M. A., Corti, C., & Razzetti, E. (2007). *Fauna d'Italia, Vol. 42, Amphibia.* Bologna: Calderini.

Laurenti, J. N. (1768). *Specimen medicum, exhibens synopsin reptilium emendatum cum experimentis circa venena et antidota reptilium austriacorum.* Vienna: Johann Thomas von Trattner.

Linnaeus, C. (1758). *Systema Naturae, per Regna Tria Naturae, secundum Classes, Ordines, Genera, Species, cum Characteribus, Differentiis, Synonymis, Locis, tenth ed., Tomus I.* Stockholm: Laurentii Salvii.

Locatelli, E. (2005). Microtus (Terricola) arvalidens *del Bus del la Fada Nana*. Unpublished BA thesis, Università degli Studi di Ferrara.

López-García, J. M., Blain, H.-A., Bennàsar, M., Alcover, J. A., Bañuls-Cardona, S., Fernández-García, M., Fontanals, M., Martín, P., Morales, J. I., Muñoz, L., Pedro, M., & Vergés, J. M. (2014). Climate and landscape during Heinrich Event 3 in southwestern Europe: the small-vertebrate association from Galls Carboners cave (Mont-ral, Tarragona, north-eastern Iberia). *Journal of Quaternary Science, 29*(2), 130–140.

López-García, J. M., Piñero, P., Agustí, J., Furió, M., Galán, J., Moncunill-Solé, B., Ruiz-Sánchez, F. J., Blain, H.-A., Sanz, M., & Daura, J. (2024). Chronological context, species occurrence, and environmental remarks on the Gelasian site Pedrera del Corral d'en Bruach (Barcelona, Spain) based on the small-mammal associations. *Historical Biology, 36*(3), 657–676.

Loréal, E., Georgalis, G. L., & Čerňanský, A. (2024). *Pseudopus pannonicus* (Squamata), the largest known anguid lizard—Redescription of the type material and new specimens from the Neogene and Quaternary of Hungary and Poland. *The Anatomical Record, 308*(1): 45–113.

Macaluso, L., Villa, A., Pitruzzella, G., Rook, L., Pogoda, P., Kupfer, A., & Delfino M. (2020). Osteology of the Italian endemic spectacled salamanders, *Salamandrina* spp. (Amphibia, Urodela, Salamandridae): selected skeletal elements for palaeontological investigations. *Journal of Morphology, 281*(11), 1391–1410.

Macaluso, L., Villa, A., Carnevale, G., & Delfino M. (2021a). Past, present, and future climate space of the only endemic vertebrate genus of the Italian peninsula. *Scientific Reports, 11,* 22139.

Macaluso, L., Villa, A., Pitruzzella, G., Rook, L., Carnevale, G., & Delfino, M. (2021b). A progressive extirpation: an overview of

the fossil record of *Salamandrina* (Salamandridae, Urodela). *Historical Biology, 33*(12)*,* 3723–3740.

Macaluso, L., Mannion, P. D., Evans, S. E., Carnevale, G., Monti, S., Marchitelli, D., & Delfino, M. (2022). Biogeographic history of Palearctic caudates revealed by a critical appraisal of their fossil record quality and spatio-temporal distribution. *Royal Society Open Science, 9,* 220935.

Macaluso, L., Bertini, A., Carnevale, G., Eronen, J.T., Martinetto, E., Saarinen, J., Villa, A., Capasso, F., & Delfino, M. (2023a). A combined palaeomodelling approach reveals the role as selective refugia of the Mediterranean peninsulas. *Palaeogeography, Palaeoclimatology, Palaeoecology, 625,* 111699.

Macaluso, L., Wencker, L. C. M., Castrovilli, M., Carnevale, G., & Delfino M. (2023b). A comparative atlas of selected skeletal elements of European urodeles (Amphibia: Urodela) for palaeontological investigations. *Zoological Journal of the Linnean Society, 197*(3), 569–619.

Marchetti, M., Parolin, K., & Sala, B. (2000). The Biharian fauna from Monte La Mesa (Verona, northeastern Italy). *Acta Zoologica Cracoviensia, 43*(1)*,* 79–105.

Margari, V., Roucoux, K., Magri, D., Manzi, G., & Tzedakis, P. C. (2018). The MIS 13 interglacial at Ceprano, Italy, in the context of Middle Pleistocene vegetation changes in southern Europe. *Quaternary Science Reviews, 199*, 144–158.

Mazza, P., Rustioni, M., Agostini, S., & Rossi, A. (2005). An unexpected Late Pleistocene macaque remain from Grotta degli Orsi Volanti (Rapino, Chieti, central Italy). *Geobios, 38*(2)*,* 211–217.

Mecozzi, B., Iannucci, A., Sardella, R., Curci, A., Daujeard, C., & Moncel, M. H. (2021). *Macaca* ulna from new excavations at the Notarchirico Acheulean site (Middle Pleistocene, Venosa, southern Italy). *Journal of Human Evolution, 153,* 102946.

Meulen, A. J. van der (1973). Middle Pleistocene smaller mammals from the Monte Peglia (Orvieto, Italy), with special reference to the phylogeny of *Microtus* (Arvicolidae, Rodentia). *Quaternaria, 17,* 1–44.

Nasrabadi, R., Rastegar-Pouyani, N., Rastegar-Pouyani, E., Kami, H. G., Gharzi, A., & Hosseinian Yousefkhani, S. S. (2018a). Distribution and environmental suitability of the European glass lizard *Pseudopus apodus* (Pallas, 1775) in the Iranian Plateau. *Russian Journal of Herpetology, 25*(1)*,* 6–10.

Nasrabadi, R., Rastegar-Pouyani, N., Rastegar-Pouyani, E., Kami, H. G., Gharzi, A., & Hosseinian Yousefkhani, S. (2018b). The effects of climate change on the distribution of European glass lizard *Pseudopus apodus* (Pallas, 1775) in Eurasia. *Ecological Research, 33*(1)*,* 199–204.

Oliveira, D., Desprat, S., Yin, Q., Rodrigues, T., Naughton, F., Trigo, R. M., Su, Q., Grimalt, J. O., Alonso-Garcia, M., Voelker, A. H. L., Abrantes, F., & Sánchez Goñi, M. F. (2020). Combination of insolation and ice-sheet forcing drive enhanced humidity in northern subtropical regions during MIS 13. *Quaternary Science Reviews, 247*, 106573.

Oppel, M. (1811). *Die Ordnungen, Familien und Gattungen der Reptilien, als Prodrom einer Naturgeschichte derselben.* Munich: Joseph Lindauer.

Peretto, C., Arnaud, J., Moggi-Cecchi, J., Manzi, G., Nomade, S., Pereira, A., Falguères, C., Bahain, J. J., Grimaud-Hervé, D., Berto, C., Sala, B., Lembo, G., Muttillo, B., Gallotti, R., Hohenstein, U. T., Vaccaro, C., Coltorti, M., & Arzarello, M. (2015). A human deciduous tooth and new 40Ar/39Ar dating results from the Middle Pleistocene archaeological site of Isernia La Pineta, Southern Italy. *PLoS ONE, 10*(10)*,* e0140091.

Rafinesque, C. S. (1815). *Analyse de Nature, ou Tableau de l'Universe et des Corps Organisés.* Palermo: Jean Barravecchia.

Ratnikov, V. (2001). Osteology of Russian toads and frogs for paleontological researches. *Acta Zoologica Cracoviensia, 44*(1)*,* 1–23.

Ratnikov, V. (2024). Do northern species of amphibians and reptiles of Eurasia need southern refugia? *Biological Journal of the Linnean Society, 141*(2)*,* 169–183.

Ratnikov, V. Yu., & Litvinchuk, S. N. (2007). Comparative morphology of trunk and sacral vertebrae of tailed amphibians of Russia and adjacent countries. *Russian Journal of Herpetology, 14*(3), 177–190.

Rifai, L., Abu Baker, M., Al Shafei, D., Disi, A., Mahasneh, A., & Amr, Z. (2005). *Pseudopus apodus* (Pallas, 1775) from Jordan, with notes on its ecology. *Herpetozoa, 18*(3/4)*,* 133–140.

Roček, Z. (1980). The dentition of the European glass lizard *Ophisaurus apodus* (Pallas, 1775) (Reptilia, Sauria: Anguidae), with notes on the pattern of tooth replacement. *Amphibia-Reptilia, 1*(1)*,* 19–27.

Roček, Z. (2019). A contribution to the herpetofauna from the late Miocene of Gritsev (Ukraine). *Comptes Rendus Palevol, 18*(7)*,* 817–847.

Russo Ermolli, E., Di Donato, V., Martín-Fernández, J. A., Orain, R., Lebreton, V., & Piovesan, G. (2015). Vegetation patterns in the Southern Apennines (Italy) during MIS 13: Deciphering pollen variability along a NW-SE transect. *Review of Palaeobotany and Palynology, 218*, 167–183.

Sala, B., & Masini, F. (2007). Late Pliocene and Pleistocene small mammal chronology in the Italian peninsula. *Quaternary International, 160*(1), 4–16.

Salzani, L., & Sauro, U. (2003). Bosco Chiesanuova. Indagini archeologiche nella grotta della Fada Nana. *Quaderni di archeologia del Veneto, 19*, 93–94.

Sanchiz, B. (1998). Salientia. In P. Wellnhofer (Ed.), *Handbuch der Paläoherpetologie, Part 4* (pp. 1–275). Munich: Verlag Dr. Friedrich Pfeil.

Sauro, U., & Zorzi, F. (2017). Problematic karst fillings of late lower Pleistocene age in a cave of the Lessini Mountains (Venetian Fore Alps, Verona). *Alpine and Mediterranean Quaternary, 30*(1), 75–86.

Sauro, U., Salzani, L., Salzani, P., Fasani, L., & Cozza, F. (2007). Ritrovamenti dell'Età del Rame sui Lessini. Indagini archeologiche in due grotticelle del Vajo di Squaranto (Bosco Chiesanuova). *Bollettino del Museo Civico di Storia Naturale di Verona, 31*, 99–128.

Seghetti, S. M., Villa, A., Tschopp, E., Bernardini, F., Laddaga, L., Fanelli, M., Levi, R., & Delfino, M. (2020). Skull osteology of *Vipera walser* (Squamata, Viperidae): description, variability, ontogeny, and diagnostic characters in comparison to other Italian vipers. *Journal of Morphology, 282*(1)*,* 5–47.

Sillero, N., Campos, J., Bonardi, A., Corti, C., Creemers, R., Crochet, P.-A., Crnobrnja Isailović, J., Denoël, M., Ficetola, G. F., Gonçalves, J., Kuzmin, S., Lymberakis, P., de Pous, P., Rodríguez, A., Sindaco, R., Speybroeck, J., Toxopeus, B., Vieites, D. R., & Vences, M. (2014). Updated distribution and biogeography of amphibians and reptiles of Europe. *Amphibia-Reptilia, 35*(1)*,* 1–31.

Sindaco, R., Doria, G., Razzetti, E., & Bernini, F. (2006). *Atlante degli Anfibi e dei Rettili d'Italia / Atlas of Italian Amphibians and Reptiles.* Firenze: Edizioni Polistampa.

Sorbelli, L., Villa, A., Gentili, S., Cherin, M., Carnevale, G., Tschopp, E., & Delfino, M. (2021). The Early Pleistocene ectothermic vertebrates of Pietrafitta (Italy) and the last Western European occurrence of *Latonia* Meyer, 1843. *Comptes Rendus Palevol, 20*(26)*,* 555–583.

Speybroeck, J., Beukema, W., Bok, B., & Van der Voort, J. (2016). *Field guide to the amphibians and reptiles of Britain and Europe.* London: Bloomsbury Publishing.

Stojanov, A., Tzankov, N., & Naumov, B. (2011). *Die Amphiben und Reptilien Bulgariens.* Frankfurt: Chimaira.

Strani, F., Sardella, R., & Mecozzi, B. (2021). An overview of the Middle Pleistocene in the north Mediterranean region. *Alpine and Mediterranean Quaternary, 34*(1)*,* 5–16.

Szyndlar, Z. (1984). Fossil snakes from Poland. *Acta Zoologica Cracoviensia, 28*(1), 1–156.

Szyndlar, Z. (1991a). A review of Neogene and Quaternary snakes of Central and Eastern Europe. Part I: Scolecophidia, Boidae, Colubrinae. *Estudios Geológicos, 47*(1–2)*,* 103–126.

Szyndlar, Z. (1991b). A review of Neogene and Quaternary snakes of Central and Eastern Europe. Part II: Natricinae, Elapidae, Viperidae. *Estudios Geológicos, 47*(3–4)*,* 237–266.

Szyndlar, Z., & Schleich, H. H. (1993). Description of Miocene snakes from Petersbuch 2 with comments on the lower and middle Miocene ophidian faunas of southern Germany. *Stuttgarter Beiträge zur Naturkunde, Serie B, 192,* 1–47.

Telenchev, I., Simeonovska-Nikolova, D., Natchev, N., & Tzankov, N. (2015). A preliminary study on the habitat selection of European glass lizard (*Pseudopus apodus*) in southeast Bulgaria. *Annuaire de l'Université de Sofia "St. Kliment Ohridski", Faculte de Biologie, 4,* 280–290.

Tzedakis, P. C., Hooghiemstra, H., & Pälike, H. (2006). The last 1.35 million years at Tenaghi Philippon: revised chronostratigraphy and long-term vegetation trends. *Quaternary Science Reviews, 25*, 3416–3430.

Venczel, M. (2000). *Quaternary snakes from Bihor (Romania).* Oradea: Tării Crişurilor Museum.

Villa, A., & Delfino, M. (2019). A comparative atlas of the skull osteology of European lizards (Reptilia: Squamata). *Zoological Journal of the Linnean Society, 187*(3), 829–928.

Villa, A., Tschopp, E., Georgalis, G. L., & Delfino, M. (2017). Osteology, fossil record and palaeodiversity of the European lizards. *Amphibia-Reptilia, 38*(1)*,* 79–88.

Villa, A., Blain, H.-A., & Delfino, M. (2018a). The Early Pleistocene herpetofauna of Rivoli Veronese (Northern Italy) as evidence for humid and forested glacial phases in the Gelasian of Southern Alps. *Palaeogeography, Palaeoclimatology, Palaeoecology, 490,* 393–403.

Villa, A., Blain, H.-A., Hoek Ostende, L.W. van den, & Delfino, M. (2018b). Fossil amphibians and reptiles from Tegelen (Province of Limburg) and the early Pleistocene palaeoclimate of The Netherlands. *Quaternary Science Reviews, 187,* 203–219.

Villa, A., Bacciotti, M., Sala, B., & Delfino, M. (2020a). Early Biharian amphibians and reptiles from Monte La Mesa (Verona, northeastern Italy): a typical herpetological assemblage from the Early Pleistocene of Veneto. *Bollettino della Società Paleontologica Italiana, 59*(2)*,* 85–104.

Villa, A., Bon, M., & Delfino, M. (2020b). Trapped in a Roman well: amphibians and reptiles from Tenuta Zuccarello near Marcon, Venice, Italy. *Historical Biology, 32*(1)*,* 55–70.

Villa, A., Minnelli, E., Bona, F., Bellucci, L., Sardella, R., & Delfino, M. (2021). The amphibians and reptiles from the Early Pleistocene of Coste San Giacomo (Anagni Basin, Italy). *Historical Biology, 33*(11)*,* 3075–3083.

Wagler, J. (1830). *Natürliches System der Amphibien, mit vorangehender Classification der Säugthiere und Vogel. Ein Beitrag zur vergleichenden Zoologie.* Munich: J.G. Cotta.

Wilson, D. E., Mittermeier, R. A., & Lacher, T. E. (2017). *Handbook of the Mammals of the World – Volume 7 Rodents II.* Barcelona: Lynx Nature Books.

Zaher, H., Grazziotin, F. G., Cadle, J. E., Murphy, R. M., Cesar de Moura-Leite, J., & Bonatto, S. L. (2009). Molecular phylogeny of advanced snakes (Serpentes, Caenophidia) with an emphasis on South American Xenodontines: a revised classification and descriptions of new taxa. *Papéis Avulsos de Zoologia, 49*(11), 115–153.

Zahradnicek, O., Horacek, I., & Tucker, A. S. (2008). Viperous fangs: Development and evolution of the venom canal. *Mechanisms of Development, 125*(9–10)*,* 786–796.

Publisher's Note Springer Nature remains neutral with regard to jurisdictional claims in published maps and institutional affiliations.